CURVED DESCENDING LANDING APPROACH GUIDANCE AND CONTROL

By

Daniel J. Crawford

B.S. Physics, University of Massachusetts

1961

A Thesis Submitted to

The Faculty of

The School of Engineering and Applied Science

of The George Washington University in partial satisfaction

of the requirements for the degree of Master of Science

December 1974

Thesis directed by

Roland L. Bowles

Assistant Professorial Lecturer in Engineering

ACKNOWLEDGMENTS

My deepest appreciation is extended to all those whose efforts contributed to this document. I am indebted to the National Aeronautics and Space Administration for allowing me the time and opportunity to conduct this study. Words of thanks are due to Mr. M. K. Morin for his encouragement and administrative guidance and to Mr. James E. Dieudonne for his help in the technical editing of the paper. I would also like to thank Mrs. Shirley Adams, Mrs. Ann Walker, and Mr. Tom Whiteway for their help in preparing the manuscript. Finally, I am deeply grateful to Dr. Roland L. Bowles, chairman of my advisory committee, for his advice in organizing the study and for his suggestions in presenting the results.

ABSTRACT

Linear optimal regulator theory is applied to a nonlinear simulation of a transport aircraft performing a helical landing approach. A closed form expression for the quasi-steady nominal flight path is presented along with the method for determining the corresponding constant nominal control inputs. The Jacobian matrices and the weighting matrices in the cost functional are time varying. A method of solving for the optimal feedback gains is reviewed. The control system is tested on several alternative landing approaches using both three and six degree flight path angles. On each landing approach, the aircraft was subjected to large random initial state errors and to randomly directed crosswinds. The system was also tested for sensitivity to changes in the parameters of the aircraft and of the atmosphere. Performance of the optimal controller on all the three degree approaches was very good, and the control system proved to be reasonably insensitive to parametric uncertainties. It did not perform as well on the six degree approaches, and a modification to these flight paths is proposed for the purpose of improving performance.

TABLE OF CONTENTS

LIST OF TABLES

LIST OF FIGURES

LIST OF SYMBOLS

A, A(t)	state coefficient matrix (6x6) in linearized equations of motion.
B, B(t)	control coefficient matrix (6x3) in linearized equations of motion.
C_D	total drag coefficient.
C_{D_0}	drag coefficient for zero lift.
C_L	total lift coefficient.
C_{L_α}	$\partial C_L / \partial \alpha$, deg^{-1}.
D	aerodynamic drag force, N.
$\bar{f}$, $\bar{f}(\bar{x},\bar{u})$	derivative of the state vector, x, (6x1).
$\bar{f}_1$	vector function, (3x1), used in determining nominal open loop control for equilibrium.
g	gravitational force per unit mass= 9.80 m/s^2.
h	altitude, -z, m.
H	Hamiltonian of linearized system.
J	cost functional, performance index.
K, K(t)	feedback gain matrix, (3x6).
$K_{i,j}$	i,j element of K.
L	aerodynamic lift force, N.
m	mass of aircraft, kg.
M	weighting matrix (6x6) on terminal state variations.
$\bar{p}$, $\bar{p}(t)$	vector, (6x1), of costates.
q	dynamic pressure, N/m^2.

Q	weighting matrix (6x6) on state variations.
r	radius of helix, m.
R	weighting matrix (3x3) on control variations.
S	reference wing area of aircraft, m^2.
S_1, $S_1(t)$	matrix (6x6) relating the costates to the states in equation (30). Solution of the time varying matrix Riccati equation.
t	time, independent variable, s.
T	total engine thrust, N.
T/m	thrust to mass ratio, m/s^2.
T_γ	orthogonal transformation (3x3) through the angle γ.
T_ϕ	orthogonal transformation (3x3) through the angle ϕ.
T_ψ	orthogonal transformation (3x3) through the angle ψ.
$\bar{u}$	control vector (3x1).
V	scalar speed of the aircraft, m/s.
$\bar{V}$	velocity vector (3x1) resolved along rotating axes system.
V_w	scalor magnitude of crosswinds, m/s.
x	displacement of aircraft in the north-south direction relative to the origin of the fixed axes system, m.
$\bar{x}$	state vector (6x1) of the system.
y	displacement of aircraft in the east-west direction relative tc the origin of the fixed axes system, m.
z	vertical displacement of aircraft relative to the origin of the fixed axes system, m.

Z, $Z(t)$	state coefficient matrix (12x12) in equation 26.
α	angle of attack, deg.
α_0	angle of attack for zero lift, deg.
γ	flight path angle, rad.
$\overline{\delta u}$	variation from nominal control vector (3x1).
$\overline{\delta x}$	variation from nominal state vector (6x1).
η	aerodynamic efficiency factor in equation 6.
ρ, $\rho(h)$	density of air, kg/m^3.
ϕ	aircraft roll angle, rad.
ψ	aircraft track angle, rad.
ψ_w	direction of wind, rad.
$\bar{\omega}$	rotation vector of aircraft (3x1) resolved along rotating axes system.
Ω, $\Omega(t,h)$	transition matrix (12x12) for the combined system of states and costates in equation 28.
$\Omega_{i,j}$	submatrices (6x6) of Ω.
δx_m, δy_m δz_m, δV_m $\delta \gamma_m$, $\delta \psi_m$	symbols used in defining the diagonal elements of the M weighting matrix.
δx_Q, δy_Q δz_Q, δV_Q $\delta \gamma_Q$, $\delta \psi_Q$	symbols used in defining the diagonal elements of the Q weighting matrix.

$\delta\alpha_R$, $\delta\phi_R$ $\delta(T/m)_R$	symbols used in defining the diagonal elements of the R weighting matrix.

Subscripts:

0	initial value.
f	final value.
N	nominal value.
SI	nominal value when the aircraft executes roll-out maneuver.

Operators:

$\int_a^b (\ )dt$	definite integration with respect to time.
$\dot{(\ )}$	derivitive with respect to time.
$\frac{d(\ )}{da}$	derivitive with respect to a.
$\frac{\partial(\ )}{\partial a}$	partial derivitive with respect to a.
$\bar{a} \times \bar{b}$	cross product of a and b.
$(\ )^{-1}$	inverse of matrix.
$(\ )^T$	transpose of matrix or vector.
$u\left[a,b\right]$	uniformly distributed random variable with range (a,b).

INTRODUCTION

Aircraft traffic in the neighborhood of commercial airports has been the subject of intensive study during the past several years. Noise, collision avoidance, airspace congestion, air pollution, and dangerous wing tip vortices are all problems which are being studied by engineers today. In the present scheme, aircraft are typically sequenced to follow one another down a three degree flight path on a straight-in approach to the runway. This path very often results in low altitude flying at relatively high power settings over residential or densely populated business districts which is objectionable, at least from a noise standpoint if not from the standpoint of safety. Recently, steeper, six degree flight paths and two segment approaches (Ref. 12) have been proposed to eliminate these problems and are currently being tested. This paper proposes an alternative to these landing approaches. It consists of descent along a helical path to a low altitude where the straight-in approach is intercepted and followed. This flight path has the advantage of keeping the aircraft at low power and at relatively high altitude except in the immediate area of the airport. The helical path is quasi-steady in that the flight path angle and velocity are maintained constant during descent and the control inputs are fixed except to null flight path errors.

Implementation of the proposed automatic guidance system requires two factors which are not at present universally available. The two factors are an on-board flight control computer and a fairly precise knowledge of the aircraft's position in space. However, with the advent of automatic landing systems, flight computers are becoming much more common on commercial transports and the current installation of the microwave landing system (MLS) equipment at airports throughout the country will make the necessary position data available (Ref. 12).

The method proposed in this paper uses the theory of optimum control which is treated in references 1 through 5. The theory is applied to a three degree of freedom nonlinear aircraft simulation. In order to pose the problem as a linear regulator, the equations were linearized about a nominal state (helical path) and control trajectory. The resulting near optimum feedback control gains were then tested in the nonlinear model. This work is an extension of that presented in references 6 and 8. The extension includes increasing the number of states to six and the number of controls to three. The additional states removes the restriction that altitude be monotonically decreasing and the inclusion of thrust, autothrottle, as a control, allows treatment of aircraft other than gliders. Reference 6 concerns itself with a HL-10 lifting body reentry vehicle and reference 8 with an unpowered Boeing 707 with no external wind

disturbances. Another extension of this work is inclusion of the quasi-steady helical path with its consequent piecewise constant control inputs. This factor greatly reduces the problem of computer storage of the state and control trajectories. The method for computing these quasi-steady paths along with the method for computing appropriate control inputs are presented here. In addition, a derivation of the equations of motion is given, along with the method of solving for the near optimum feedback gains. It should be noted that this study, as do references 6 and 8, uses angle of attack and bank angle as control inputs. This is a simplification of the dynamic model which does not include control surfaces such as elevators, ailerons, or rudder.

Feedback gains were obtained for several candidate approach paths including both three and six degree flight path angles and turns of 180, 270, and 360 degrees. An overhead approach was the principal path studied, i.e. one in which the aircraft crossed over the runway at a ninety degree angle heading east at an altitude of 550 meters. At about 1800 meters east of the runway center line it intercepted the helix and descended down it, making a total turn, to the right, of 270 degrees. The turn was completed at an altitude of 100 meters where the aircraft intercepted the straight-in approach. At this time, it was about 1900 meters from the touchdown point on the runway. The plane continued to descend until, at twelve meter altitude, it

executed a flare maneuver. The effectiveness of the control system was tested in the nonlinear simulation by introducing initial errors in the states, crosswinds, and uncertainties in the aerodynamics of the aircraft.

The aircraft treated in the study is a Boeing 737-100, which is a two engined small commercial transport used for relatively short haul flights. Langley Research Center has recently procured one of these aircraft from Boeing and it is being used to study and test advanced automatic control and avionics concepts in the neighborhood of the air terminal. Whereas the results presented in this paper show feasibility, it is hoped that they will be applied first to a more sophisticated six degree of freedom simulation of the aircraft, and then eventually to be tested on the aircraft itself.

ANALYSIS

Introduction

The purpose of this section is to present the mathematics involved in simulating the aircraft and in implementing the feedback control law. Notice that in figure 1, the aircraft is modeled by a set of six nonlinear ordinary differential equations represented by the single vector equation

$$\dot{\bar{x}} = \bar{f}(\bar{x},\bar{u},t) \qquad (1)$$

This set of equations was integrated numerically using a fixed step fourth order Runge Kutta algorithm. The feedback control law used in this study requires that the nominal state trajectories, $\bar{x}_n$, the nominal control time histories, $\bar{u}_n$, and the feedback gain matrix, K, be stored in an on-board computer. However, it will be shown that by choosing particular nominal trajectories, the vector $\bar{u}_N$ changes only twice, and the vector $\bar{x}_N$ is a simply computed analytic vector function of time. This eliminates some of the on-board storage requirements and makes the control system simpler and more flexible.

As simulated, the aircraft has six state variables and three control inputs defined as

$$\bar{x} = [x\ y\ z\ V\ \gamma\ \psi]^T$$

$$\bar{u} = [\alpha\ \phi\ T/m]^T$$

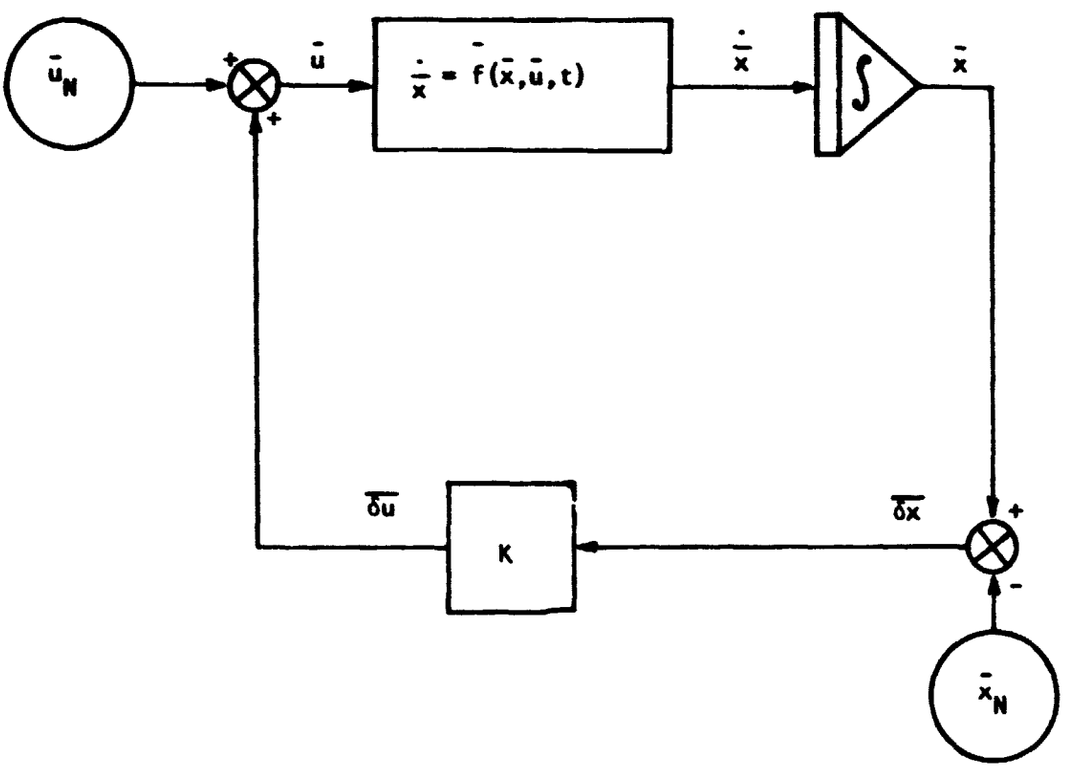

Figure 1.- Schematic Diagram of Aircraft Landing Simulation.

The state vector $\bar{x}$ is made up of the variables x, y, and z describing the aircraft's position; V, its velocity; γ, its flight path angle; and ψ, its track angle. The control vector $\bar{u}$ is made up of the angle of attack, α; the roll angle, ϕ; and the ratio of engine thrust to aircraft mass, T/m. The two perturbation vectors $\bar{\delta x}$ and $\bar{\delta u}$, shown in figure 1, are defined as

$$\bar{\delta x} = \bar{x} - \bar{x}_n$$

$$\bar{\delta u} = \bar{u} - \bar{u}_n$$

However, in practice, $\bar{\delta u}$ is computed as:

$$\bar{\delta u} = K\bar{\delta x} \qquad (2)$$

where K is a 3x6 time varying gain matrix. This gain matrix is the solution of the regulator problem which results from linearizing equation 1 about the nominal flight path and control vector, and it is precomputed for a particular nominal flight path. This linearization yields:

$$\dot{\bar{\delta x}} = A(t)\bar{\delta x} + B(t)\bar{\delta u} = [A(t)+B(t)K(t)]\bar{\delta x} \qquad (3)$$

where $A(t) = \frac{\partial \bar{f}}{\partial \bar{x}}$ evaluated at $\bar{x} = \bar{x}_n$ and $\bar{u} = \bar{u}_n$ and $B(t) = \frac{\partial \bar{f}}{\partial \bar{u}}$ evaluates at $\bar{x} = \bar{x}_n$ and $\bar{u} = \bar{u}_n$. A is a 6x6 matrix and B is a 6x3 matrix. A statement of the regulator problem is then to find K in equations 2 and 3 which minimizes deviations of the states from their nominal values by using controls which stay within acceptable limits. More formally, the problem is to determine K which minimizes the quadratic performance index J given by

$$J = \frac{1}{2}\bar{\delta x}^T(t_f)M\bar{\delta x}(t_f) + \frac{1}{2}\int_0^{t_f} [\bar{\delta x}(t)^T Q\bar{\delta x}(t) + \bar{\delta u}(t)^T R\bar{\delta u}(t)]dt \qquad (4)$$

subject to the constraints of equation (3). M, Q, and R are weighting matrices.

Equations of Motion

The inertial axes system (x, y, z) has its origin at the desired touchdown point on the runway. The x axis is parallel to the runway and is positive in the direction of landing. The y axis is horizontal, perpindicular to the x axis and is positive to the right. The vertical z axis is perpindicular to both x and y, and is positive downward. The aircraft is treated as a point mass, subject to the forces of gravity, engine thrust, and aerodynamic lift and drag. The rotating axis system associated with the aircraft is chosen such that its x axis is always alined with the aircraft's velocity vector. Two Euler angle transformations relate the inertial axis system to the rotating axis system. They are

$$T\psi = \begin{bmatrix} \cos\psi & \sin\psi & 0 \\ -\sin\psi & \cos\psi & 0 \\ 0 & 0 & 1 \end{bmatrix}$$

and

$$T\gamma = \begin{bmatrix} \cos\gamma & 0 & \sin\gamma \\ 0 & 1 & 0 \\ -\sin\gamma & 0 & \cos\gamma \end{bmatrix}$$

These rotations are shown in Figure 2. This axes system does not roll with the aircraft. Therefore, the y body axis remains horizontal and the z body axis stays in a vertical plane with the velocity vector. The rotation vector resolved along the rotating axes system is

$$\bar{\omega} = [\dot{\psi} \sin\gamma, -\dot{\gamma}, \dot{\psi} \cos\gamma]^T$$

and the velocity vector is

$$\bar{V} = [V \quad 0 \quad 0]^T$$

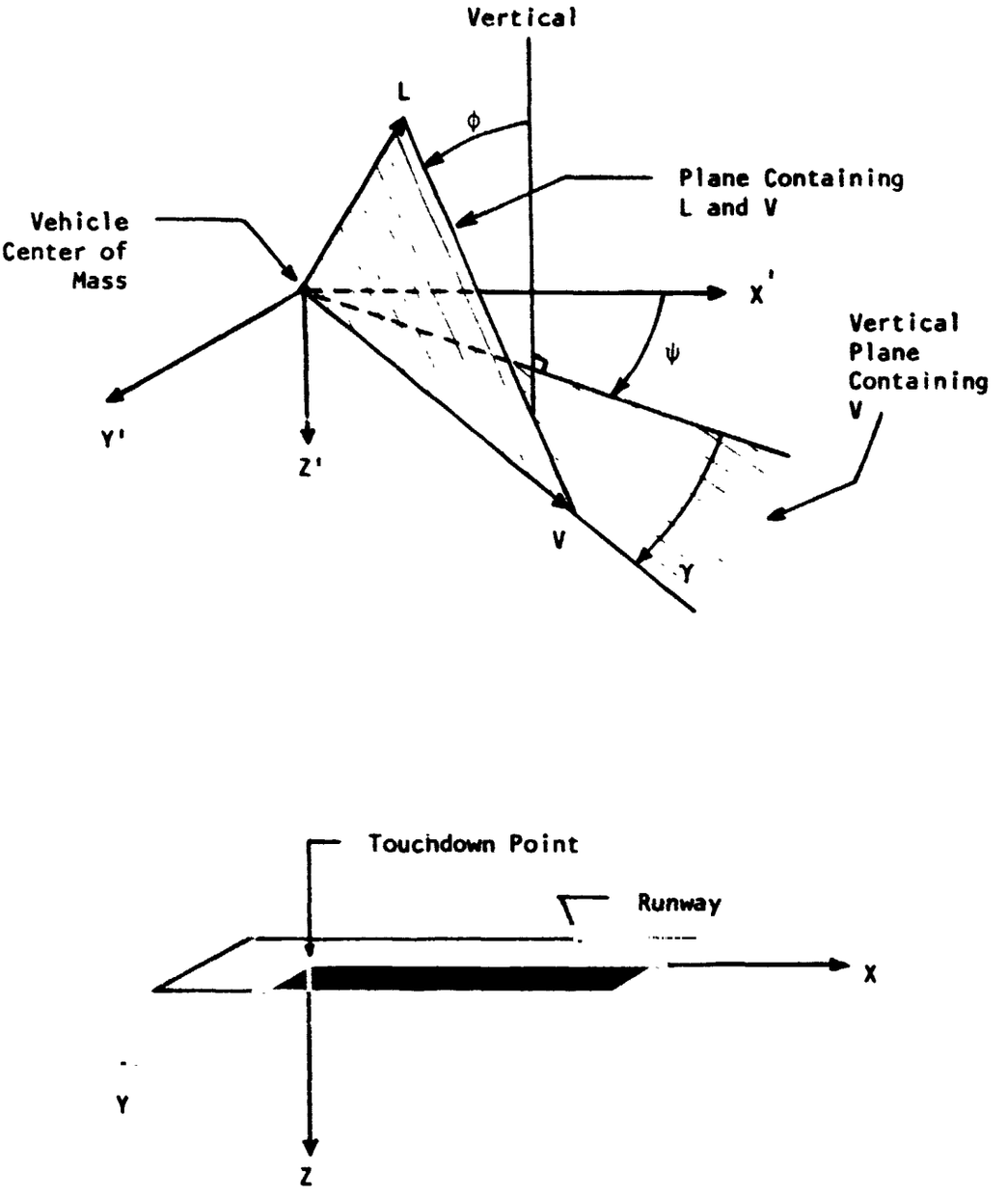

Figure 2.- Rotating Axis System.

The forces acting on the aircraft resolved along the rotating axes are

$$\text{Drag} = [-D \quad 0 \quad 0]^T$$

$$\text{Thrust} = [T\cos\alpha \quad 0 \quad -T\sin\alpha]^T$$

$$\text{Gravity} = T_\gamma T_\psi [0 \quad 0 \quad mg]^T$$

$$\text{Lift} = T_\phi [0 \quad 0 \quad -L]^T$$

where $T_\phi = \begin{bmatrix} 1 & 0 & 0 \\ 0 & \cos\phi & -\sin\phi \\ 0 & \sin\phi & \cos\phi \end{bmatrix}$

The lift force is perpendicular to the velocity and rolls with the aircraft. The transformation T_ϕ resolves this force along the y and z rotating axes. The angle of attack, α, is defined as the angle between the velocity vector and the x body axis of the aircraft. The dynamics of the aircraft are then described by equating the change in linear momentum to the sum of the applied forces

$$m(\dot{\bar{V}}+\bar{\omega}\times\bar{V}) = \text{Drag} + \text{Thrust} + \text{Gravity} + \text{Lift}$$

or

$$m\begin{bmatrix}\dot{V}\\0\\0\end{bmatrix} + m\begin{bmatrix}0\\\dot{V\psi}\cos\gamma\\\dot{V\gamma}\end{bmatrix} = \begin{bmatrix}-D\\0\\0\end{bmatrix} + \begin{bmatrix}T\cos\alpha\\0\\-T\sin\alpha\end{bmatrix} + \begin{bmatrix}mg\sin\gamma\\0\\mg\cos\gamma\end{bmatrix} + \begin{bmatrix}0\\L\sin\phi\\-L\cos\phi\end{bmatrix}$$

To facilitate integration of these equations, they are written with the derivative of the states V, ψ, and γ on the left hand side. These three equations are combined with three kinematic relations which resolve the velocity along the x, y, and z inertial axis

$$\begin{bmatrix}\dot{x}\\\dot{y}\\\dot{z}\end{bmatrix} = [T_\gamma T_\psi]^{-1}\begin{bmatrix}V\\0\\0\end{bmatrix}$$

The six equations of state are then

$$
\begin{aligned}
\dot{x} &= V \cos\gamma \cos\psi \\
\dot{y} &= V \cos\gamma \sin\psi \\
\dot{z} &= V \sin\gamma \\
\dot{V} &= -D/m + (T/m)\cos\alpha + g \sin\gamma \\
\dot{\gamma} &= -(T/mV)\sin\alpha + (g/V)\cos\gamma - (L/mV)\cos\phi \\
\dot{\psi} &= L\sin\phi/(mV\cos\gamma)
\end{aligned}
\qquad (5)
$$

Equation 5 is the expanded form of equation 1.

Aerodynamics and Aircraft Parameters

The aircraft simulated in this study is a Boeing 737-100 which is a small two-engined transport airplane designed primarily to operate from short runways over relatively short distances. It is described in references 9 and 10. The equations for the lift and drag forces are

$$L = q\,S\,C_L$$

$$D = q\,S\,C_D$$

where C_L and C_D are the coefficients of lift and drag, respectively; S is the wing reference area; and q is dynamic pressure. C_L, C_D, and q are defined as

$$
\begin{aligned}
C_L &= C_{L_\alpha}(\alpha-\alpha_o)\frac{\pi}{180} \\
C_D &= C_{D_o} + \eta[C_{L_\alpha}(\alpha-\alpha_o)\frac{\pi}{180}]^2 \qquad (6) \\
\text{and} \quad q &= 1/2\ \rho V^2
\end{aligned}
$$

The assumption of a parabolic drag polar where the induced drag is a quadratic function of the lift coefficient is not restrictive for the range of speed and angle of attack employed in this study.

Air density, ρ, was approximated by the following equation taken from reference 8.

$$\rho = 1.22[1.-(2.257\text{x}10^{-5})h]^{4.255} \qquad (7)$$

This proved to be a very good approximation to the standard atmospheric density of reference 7. The airplane was configured with the landing gear down and the flaps deployed at 40 degrees. The parameters of equation 6 (C_{L_α}, α_o, C_{D_o}, and η) were chosen to fit data on C_L and C_D provided by Boeing for this configuration. The parameters of the aircraft are listed in Table 1.

Nominal Flight Paths

The nominal path can be chosen quite arbitrarily when applying the linear regulator method to the aircraft landing problem. However, practical considerations lead one into choosing a particular class of flight paths. The most common approach used today on commercial transports is the 3° nondecelerating straight-in approach. That is, the pilot lines up with the runway and then descends at constant velocity along an equilibrium path which intersects the horizontal at an angle of 3°. The control inputs are nearly constant varying only to offset atmospheric disturbances. A mathematical description of this path is

$$\dot{\bar{x}} = [V_o\cos\gamma_o \quad 0. \quad V_o\sin\gamma_o \quad 0 \quad 0 \quad 0]^T$$

$$\bar{x}(0) = [x_o \quad 0 \quad z_o \quad V_o \quad \gamma_o \quad 0]^T$$

At approximately 12 meters altitude, the aircraft leaves this quasi-steady condition and flares in order to touch down more smoothly. This

SYMBOL	VALUE	PARAMETER DEFINITION
C_{L_α}	7.162	Lift curve slope
α_o	-10.4°	Angle of attack for zero lift
C_{D_o}	.157	Drag coefficient for zero lift
η	.0314	Efficiency factor
S	91.04 M^2	Aerodynamic reference area
m	40,823. Kg.	Mass of vehicle

TABLE 1 - Characteristics of the 737-100 (Gear Down-Flaps at 40°)

path calls for constant control inputs and because of its simplicity, it requires very little storage. If the nominal path had been chosen arbitrarily, the six states and three controls would have had to have been stored for many points along the path.

In order to relieve airport noise problems and to decrease traffic congestion in the neighborhood of the airport, various other approaches have been proposed and are being tested. These include the steeper 6° nondecelerating straight-in approach and a combination of the 6° and 3° approach. The method proposed in this paper is a quasi-steady helical approach. All other quasi-steady motions of an aircraft are special cases of this generalization. That is, the nominal path is descent along a helix from some initial altitude. The centerline of the runway is tangent to the helix and at some specified lower altitude, the aircraft follows this tangent into a straight-in approach. By making the assumption that atmospheric density is constant over the range of altitude considered, this path calls for fixed controls during the helical descent, and fixed but different control inputs during the straight-in portion. The variation in atmospheric density in this range of altitude is about four percent. The assumption of constant density is made during calculations of nominal path, nominal control inputs, and feedback gains. During the simulated flights, using the closed loop control system, atmospheric density is allowed to vary according to equation 7. The small error introduced by this assumption was nulled out by the control system as though it were an external disturbance. A more formal description of the nominal path is

$$\dot{\bar{x}} = \begin{bmatrix} V_o \cos\gamma_o \cos\psi \\ V_o \cos\gamma_o \sin\psi \\ V_o \sin\gamma_o \\ 0 \\ 0 \\ \dot{\psi}_o \end{bmatrix} \qquad x(0) = \begin{bmatrix} x_o \\ y_c \\ z_o \\ V_o \\ \gamma_o \\ \psi_o \end{bmatrix} \qquad (8)$$

for the altitude range

$$-z_{SI} \leq h \leq -z_o$$

where $-z_{SI}$ is the altitude at which the aircraft rolls into the straight-in approach. The parameters z_o, z_{SI}, V_o, γ_o, and ψ_o are chosen with some degree of latitude and they essentially determine the nominal flight path. The last three parameters, x_o, y_o, and $\dot{\psi}_o$ are functions of the first five and are chosen such that x, y, and ψ have the desired values when z equals z_{SI}. The subscript SI will be used to specify the value of a state when z equals z_{SI}. Because the origin of the axes system is at the touchdown point on the runway, the desired values of ψ_{SI} and y_{SI} are zero. In order to determine x_{SI}, it is necessary to look at the nominal path after it starts the straight-in approach. Its description is

$$\begin{aligned} \dot{\bar{x}} &= [V_o \cos\gamma_o \quad 0 \quad V_o \sin\gamma_o \quad 0 \quad 0 \quad 0]^T \\ \bar{x}(t_{SI}) &= [x_{SI} \quad 0 \quad z_{SI} \quad V_o \quad \gamma_o \quad 0]^T \end{aligned} \qquad (9)$$

During this part of the flight $\dot{x}$ and $\dot{z}$ are constant and consequently,

$$\frac{dx}{dz} = \frac{dx}{dt} \Big/ \frac{dz}{dt} = \cot\gamma_o$$

is constant. In order to touch down at the origin,

$$x_{SI} = z_{SI} \frac{dx}{dz}$$

$$x_{SI} = z_{SI}/\tan\gamma_o \tag{10}$$

Also, during the helical descent, the rate of turn, $\dot{\psi}$, and the rate of descent, $\dot{z}$, are constant. In order to have the aircraft flying in the correct direction (ψ=0) when z equals z_{SI}, it is necessary that

$$\frac{d\psi}{dz} = \frac{2\pi - \psi_o}{z_{SI} - z_o} \tag{11}$$

and since

$$\frac{d\psi}{dt} = \frac{d\psi}{dz} \frac{dz}{dt}$$

it follows that

$$\dot{\psi}_o = \left(\frac{2\pi - \psi_o}{z_{SI} - z_o} \right) V_o \sin\gamma_o \tag{12}$$

The axis of the helix is vertical at

$$(x,y) = (x_{SI}, r)$$

where the radius r is given by

$$r = 1./(\tan\gamma_o \cdot \frac{d\psi}{dz}) \tag{13}$$

and through geometrical considerations

$$x_o = x_{SI} + r \sin \psi_o \tag{14}$$

$$y_o = r(1-\cos \psi_o) \tag{15}$$

A short example may clarify these computations. Let the landing direction be north, (ψ=0), and the aircraft's original heading be east, ($\psi_o = \frac{\pi}{2}$). The velocity is 62 meters/second and the flight path angle is 3°, ($\frac{3\pi}{180}$). Initial altitude is 450 m. The aircraft descends

along a helical path to 50 m. altitude and then down a straight path to the runway. In this example,

$$z_o = -450 \text{ m.}, \quad z_{SI} = -50 \text{ m.}, \quad V_o = 62 \text{ m./sec}$$

$$\gamma_o = \frac{3\pi}{180}, \quad \psi_o = \frac{\pi}{2}$$

$$x_{SI} = z_{SI}/\tan \gamma_o = -50/\tan(\frac{3\pi}{180}) \simeq -954. \text{m.}$$

$$\frac{d\psi}{dz} = \frac{2\pi-\psi_o}{z_{SI}-z_o} = \frac{3\pi}{2(-50+450)} = \frac{3\pi}{800} \simeq .012 \text{ rad/m.}$$

$$\dot{\psi}_o = \frac{d\psi}{dz}\frac{dz}{dt} = (\frac{3\pi}{800})(62)\sin\frac{3\pi}{180} \simeq .038 \text{ rad/sec}$$

$$r = 1./(\tan\gamma_o \cdot \frac{d\psi}{dz}) = 800/(3\pi \cdot \tan\frac{3\pi}{180}) \simeq 1620.\text{m.}$$

$$x_o = x_{SI} + r \sin \psi_o \simeq -954 + (1620.)\sin(\frac{\pi}{2}) \simeq 666.\text{m.}$$

$$y_o = r(1-\cos\psi_o) = r \simeq 1620.\text{m.}$$

Integration of equation (8) gives the following state trajectories along the helix.

$$\bar{x} = \begin{bmatrix} x_o \\ y_o \\ z_o \\ V_o \\ \gamma_o \\ \psi_o \end{bmatrix} + \begin{bmatrix} (V_o\cos\gamma_o/\dot{\psi}_o)(\sin\psi-\sin\psi_o) \\ (V_o\cos\gamma_o/\dot{\psi}_o)(\cos\psi_o-\cos\psi) \\ (V_o\sin\gamma_o)t \\ 0 \\ 0 \\ \dot{\psi}_o t \end{bmatrix} \qquad (16)$$

Likewise, integration of equation (9) yields the state trajectories along the straight portion of the flight path

$$\bar{x} = \begin{bmatrix} x_{SI} \\ 0 \\ z_{SI} \\ V_o \\ \gamma_o \\ 0 \end{bmatrix} + \begin{bmatrix} V_o \cos\gamma_o (t-t_{SI}) \\ 0 \\ V_o \sin\gamma_o (t-t_{SI}) \\ 0 \\ 0 \\ 0 \end{bmatrix} \qquad (17)$$

The time for the wings level maneuver, t_{SI}, is given by

$$t_{SI} = (z_{SI}-z_o)/V_o \sin\gamma_o \qquad (18)$$

In summary, the need to integrate and store the equations of motion for the nominal path has been eliminated. Given a particular input parameter set, $[z_o, z_{SI}, V_o, \gamma_o, \psi_o]$, equations (16) and (17) yield the value of the states at any time. Five secondary parameters, $[x_{SI}, \dot{\psi}_o, x_o, y_o, t_{SI}]$, necessary to evaluate equations (16) and (17) are given as functions of the input parameters by equations (10) through (15) and equation (18).

Nominal Control Inputs

After specifying this particular class of nominal flight paths, it is necessary to make their equations of motion which are given by equations (8) and (9), agree with the equations of motion for an arbitrary path which are given by equation (5). This is accomplished by choosing the correct open loop control vector, $\bar{u}$. Because the

path is quasi-steady, that is,

$$\dot{V} = \dot{\gamma} = 0$$

$$\dot{\psi} = \dot{\psi}_o \qquad h \geq -z_{SI}$$

$$\dot{\psi} = 0 \qquad h \leq -z_{SI}$$

$\bar{u}$ is a constant vector on the spiral and a second constant on the straight-in portion. In order to make equation (5) agree with equation (8), the following equations must be satisfied.

$$\begin{aligned} &D_N/m - (T/m)\cos\alpha - g \sin \gamma_o = 0 \\ &(T/mV_o)\sin\alpha - (g/V_o)\cos\gamma_o + (L_N/mV_o)\cos\phi = 0 \\ &\dot{\psi}_o - L_N\sin\phi/(mV_o\cos\gamma_o) = 0 \end{aligned} \qquad (19)$$

In these equations,

$$L_N = q_N S C_L$$

$$D_N = q_N S C_D$$

where

$$q_N = 1/2\ \rho_N V_o^2$$

and C_L and C_D are defined in equation (6). Using the assumption of constant air density discussed earlier, an intermediate value of altitude, h_N, is chosen, and ρ_N is computed using equation (7). That is,

$$\rho_N = 1.22[1.-(2.257\text{x}10^{-5})h_N]^{4.255}$$

The open loop control, $\bar{u}$,

$$\bar{u} = [\alpha,\ \phi,\ T/m]^T$$

which is the solution of equation (19), is not unique and these equations have no closed form solution. Equation (19) is of

the form

$$\bar{f}_1(\bar{u}) = 0$$

and it was solved by the Newton-Raphson iterative method described in reference 11. This method usually requires the Jacobian matrix which is given by

$$\frac{\partial \bar{f}_1}{\partial \bar{u}} = \begin{bmatrix} [\frac{\partial D_N}{\partial \alpha} + T\sin\alpha]/m & 0 & -\cos\alpha \\ (T/mV_o)\cos\alpha + \frac{\partial L_N}{\partial \alpha}\cos\phi/(mV_o) & -L_N\sin\phi/(mV_o) & \sin\alpha/V_o \\ \frac{\partial L_N}{\partial \alpha}\sin\phi/(mV_o\cos\gamma_o) & -L_N\cos\phi/(mV_o\cos\gamma_o) & 0 \end{bmatrix}$$

where $$\frac{\partial L_N}{\partial \alpha} = q_N S \frac{\pi}{180} C_{L_\alpha}$$

and $$\frac{\partial D_N}{\partial \alpha} = 2q_N S \left(\frac{\pi}{180}\right)^2 C_{L_\alpha}^2 \eta(\alpha-\alpha_o)$$

The possibility always exists that this algorithm will converge to an undesirable value of $\bar{u}$. Physically, the smaller value of angle of attack is desired. This corresponds to the low side of the lift/drag curve. Therefore, the solution must be examined subjectively before being accepted. A practical way to avoid this problem is to start the iterative procedure close to the desired final solution. A suggested method of doing this is to make the assumption that engine thrust is alined with the velocity vector of the aircraft. With this assumption, which is in error by the size of the angle, alpha, equation (19) becomes

$$D_N/m - T/m - g\sin\gamma_o = 0$$

$$-(g/V_o)\cos\gamma_o + (L_N/mV_o)\cos\phi = 0$$

$$\dot{\psi}_o - L_N\sin\phi/(mV_o\cos\gamma_o) = 0$$

These equations have the following closed form solution which can be used as a starting point in the Newton-Raphson algorithm. The solution is

$$\begin{aligned} \phi &= \mathrm{Tan}^{-1}(V_o\dot{\psi}_o/g) \\ \alpha &= \alpha_o + (180/\pi)(mg\cos\gamma_o)/(q_N S\, C_{L_\alpha}\cos\phi) \\ T/m &= D_N/m - g\sin\gamma_o \end{aligned} \tag{20}$$

In order to solve for the open loop controls for the straight-in portion of the nominal flight path, the following equations must be satisfied. They result from making equation (5) equivalent to equation (9).

$$\begin{aligned} &D_N/m - (T/m)\cos\alpha - g\sin\gamma_o = 0 \\ &(T/mV_o)\sin\alpha - (g/V_o)\cos\gamma_o + (L_N/mV_o) = 0 \end{aligned} \tag{21}$$

Again, the Newton-Raphson algorithm is used to solve the two equations for α and T/m. The roll angle, ϕ, of course, is zero. Using the same assumption that thrust and velocity are codirectional, the following equations can be used to start the iterative procedure.

$$\begin{aligned} \alpha &= 180.mg\cos\gamma_o/(\pi qS\, C_{L_\alpha}) + \alpha_o \\ T/m &= D_N/m - g\sin\gamma_o \end{aligned} \tag{22}$$

Notice that D_N in equation 20 will have a different numerical value than D_N in equation 21. These equations used for starting the Newton-Raphson iteration procedure yield values which are very close to the final values.

Feedback Control Gains

The purpose of this section is to present a development of the solution of the linear regulator problem. References 1 through 5 all concern themselves, in part, with this problem. A statement of the problem is given by equations (1), (3), and (4), which are repeated here for convenience.

$$\dot{\bar{x}} = \bar{f}(\bar{x},\bar{u},t) \tag{1}$$

$$\dot{\overline{\delta x}} = A(t)\overline{\delta x} + B(t)\overline{\delta u} = [A+BK]\overline{\delta x} \tag{3}$$

$$J = \frac{1}{2}\overline{\delta x}^T(t_f)M\overline{\delta x}(t_f) + \frac{1}{2}\int_0^{t_f} \overline{\delta x}^T(t)Q\overline{\delta x}(t + \overline{\delta u}^T(t)R\overline{\delta u}(t)dt \tag{4}$$

A(t) and B(t) are defined as

$$A = \frac{\partial \bar{f}}{\partial \bar{x}} \qquad B = \frac{\partial \bar{f}}{\partial u}$$

M, Q, and R are weighting matrices which must be selected by the control system designer. The problem is to find the matrix K in equation (3) which minimizes the quadratic performance index of equation (4). Following the techniques of references 1 and 2, the Hamiltonian of the system is

$$H = \frac{1}{2}\overline{\delta x}^T Q\overline{\delta x} + \frac{1}{2}\overline{\delta u}^T R\overline{\delta u} + (A\overline{\delta x})^T\bar{p} + (B\overline{\delta u})^T\bar{p}$$

where $\bar{p}$ is the vector of costates. $\bar{p}$ is the solution of the differential equation

$$\dot{\bar{p}} = -\frac{\partial H}{\partial(\overline{\delta x})} = -Q\overline{\delta x} - A^T\bar{p} \tag{23}$$

Since the control is optimal, it follows that

$$\frac{\partial H}{\partial(\overline{\delta u})} = 0$$

or

$$\frac{\partial H}{\partial(\overline{\delta u})} = R\overline{\delta u} + B^T\overline{p} = 0$$

Solving this equation for $\overline{\delta u}$, we get

$$\overline{\delta u} = -R^{-1}B^T\overline{p} \tag{24}$$

Obviously, the control weighting matrix R must be nonsingular.[1]

Combining equation (24) with equation (3) yields

$$\dot{\overline{\delta x}} = A\overline{\delta x} - BR^{-1}B^T\overline{p} \tag{25}$$

Then, combining this equation with equation (23), we have the following system of equations.

$$\begin{bmatrix} \dot{\overline{\delta x}} \\ \dot{\overline{p}} \end{bmatrix} = \begin{bmatrix} A & -BR^{-1}B^T \\ -Q & -A^T \end{bmatrix} \begin{bmatrix} \overline{\delta x} \\ \overline{p} \end{bmatrix} \tag{26}$$

Applying the transversality conditions, we get the costate vector $\overline{p}(t)$ at the final time, t_f.

$$\overline{p}(t_f) = \frac{1}{2}\frac{\partial \overline{\delta x}^T M \overline{\delta x}}{\partial \overline{\delta x}(t_f)} = M\overline{\delta x}(t_f) \tag{27}$$

The system represented in equation (26) has twelve states. Since there are six initial conditions on $\overline{\delta x}$, and six final boundary values on $\overline{p}$, this system has a unique solution.

If equation (26) is rewritten as

$$\begin{bmatrix} \dot{\overline{\delta x}} \\ \dot{\overline{p}} \end{bmatrix} = Z \begin{bmatrix} \overline{\delta x} \\ \overline{p} \end{bmatrix}$$

and if we assume that Z is constant over a small interval of time, [t,t+h], then we can write the transition equation of the system as

---

[1]Reference 1 shows that M, Q, and R must be symetric; that M and Q must be at least positive semidefinite; and that R must be positive definite.

$$\begin{bmatrix} \overline{\delta x}\ (t+h) \\ \overline{p}\ (t+h) \end{bmatrix} = \Omega(t,h) \begin{bmatrix} \overline{\delta x}(t) \\ \overline{p}(t) \end{bmatrix} \tag{28}$$

where

$$\Omega(t,h) = e^{z(t)h} = \begin{bmatrix} \Omega_{11} & \Omega_{12} \\ \Omega_{21} & \Omega_{22} \end{bmatrix} \tag{29}$$

A further assumption is made that the costates are linearly related to the states; that is,

$$\overline{p}(t) = S_1 \overline{\delta x}(t) \tag{30}$$

This assumption is proven to be true in reference 1. A comparison of equation (27) and (30) shows that

$$S_1(t_f) = M \tag{31}$$

Combining equations (28), (29), and (30) yields a transition equation for S_1

$$\begin{bmatrix} \overline{\delta x}(t+h) \\ S_1(t+h)\overline{\delta x}(t+h) \end{bmatrix} = \Omega(t,h) \begin{bmatrix} \overline{\delta x}(t) \\ S_1(t)\overline{\delta x}(t) \end{bmatrix}$$

$$S_1(t+h)[\Omega_{11}+\Omega_{12}S_1(t)]\overline{\delta x}(t) = [\Omega_{21}+\Omega_{22}S_1]\overline{\delta x}(t)$$

or

$$S_1(t+h) = [\Omega_{21}+\Omega_{22}S_1(t)][\Omega_{11}+\Omega_{12}S_1(t)]^{-1} \tag{32}$$

Reference 1 proves that this inverse does exist.

Using the difference equation (32) with the final value of the matrix S_1 given by equation (31), we can proceed backward in time and obtain S_i for all $t\varepsilon[t_o,t_f]$. At each point in time, it is necessary to compute $\Omega(t,h)$ as a function of A(t), B(t), R, and Q, using equations

(26) through (29). The gain matrix K(t) is obtained by combining equations (30) and (24).

$$\overline{\delta u} = -R^{-1}B^{T}S_{1}\overline{\delta x}(t)$$

or

$$K(t) = -R^{-1}B^{T}S_{1} \qquad (33)$$

Implementation

The landing approach guidance scheme proposed in this paper would be implemented in the following manner.

1. For a particular nominal flight path, the control system designer, after extensive analysis and testing, chooses weighting matrices M, Q, and R for the performance index in equation (4).

2. The state trajectories on the nominal flight path are then computed using equations (10) through (18).

3. The nominal open loop control inputs are then computed using the Newton-Raphson algorithm to solve equations (19) and (21). This iterative procedure is started with the values given in equations (20) and (22), respectively.

4. The Jacobian matrices A(t) and B(t) used in equation (3) are computed according to equations (A-1) and (A-2) in appendix A. Equation (3) represents the linearization of equation (1) about the nominal trajectory and control.

5. The feedback gain matrix K is computed as a function of time using equations (26) through (33).

6. In the computer aboard the aircraft are stored the time histories of the nominal flight path, the nominal control inputs, and the

feedback gains. Alternatively, the algorithm, equations (16) and (17), which computes the state trajectories is stored.

7. The aircraft, or simulated aircraft, is flown into a window; i.e., a region of state space which is 'close' to the initial states of the nominal flight path.

8. When the plane enters the window, it is switched on to the automatic landing system. It is assumed that the aircraft is receiving the necessary position data from the ground based airport landing system and receives control surface positions from transducers. This is considered time zero with respect to the nominal path.

9. The control system smoothly nulls the state errors and brings the aircraft safely onto the nominal flight path well before reaching the decision altitude.

RESULTS AND DISCUSSION

Flight Paths

In this study, the control system was tested along seven different nominal flight paths. The paths differed in initial altitude, initial heading angle, and in angle of descent. Flight paths 1, 2, and 3 are depicted in Figure 3. They all have a three degree angle of descent (flight path angle) and are initially headed north, east, and south, respectively. Flight path 1 is the easiest path to fly because its initial altitude is the highest and there is more time to null out initial errors in the state variables. Conversely, flight path 3 is the most difficult since its initial altitude is 150 meters below flight path 2 and 300 meters below flight path 1. The aircraft makes a descending turn to the right of 360, 270, and 180 degrees for flight paths 1, 2, and 3, respectively at which point it is headed north toward the runway. At this position (roll out) on the path, the aircraft is at 100 meters altitude and it rolls to a wing level attitude. It then descends in a straight line toward the runway. The flare maneuver would be executed at twelve meter altitude for the purpose of softening the impact at touchdown. Because this simulation did not include ground effects, it was terminated just above the flare altitude and off nominal errors recorded at that point.

Flight paths 1A, 2A, and 3A had the same initial altitude and heading angle respectively as flight paths 1, 2, and 3. However, they had a descent angle of six degrees rather than three. These

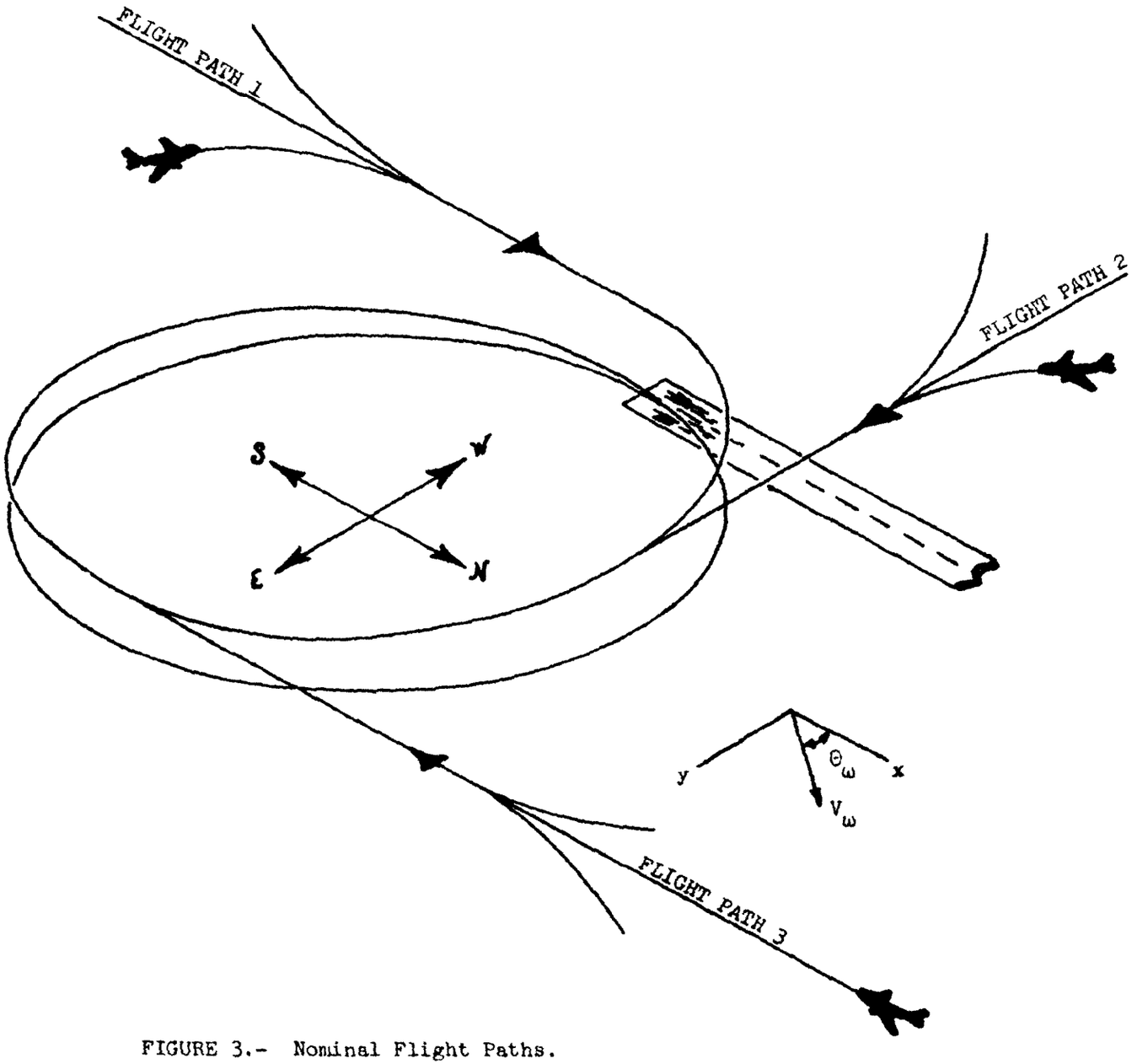

FIGURE 3.- Nominal Flight Paths.

flight paths are more difficult to fly than the first three. The rate of descent and roll angle are about doubled and the turning radius and flight time are about halved. The rollout altitude was maintained at 100 meters. These flight paths require more severe control inputs than the first three and they have less time to null off-nominal errors.

Flight path 3B is a variation of 3A. The initial altitude and rollout altitude were raised 100 meters. This had the effect of moving the helix back from the runway and about doubling the time spent on the straight-in portion of the path. Parameters of the seven flight paths are given in table 2.

Design Considerations

The control task presented here differs from conventional landing approach schemes in that errors are taken with respect to a moving point in state space rather than a fixed line. Thus, even if the aircraft were flying on the correct helical path with the correct attitude, the fact that it was late or early in time would indicate to the control system that there were state errors; in this context, the proposed guidance scheme can be considered 4-D. At crowded airports, more precise control of time sequencing should prove advantageous.

Because the feedback gain matrix K is computed automatically in a near optimum fashion, the designer's job is to choose the weighting matrices M, Q, and R of equation 4 and then to evaluate the subsequent performance of the control system. In fact, this becomes an iterative

FLIGHT PATH	INITIAL ALTITUDE	ROLLOUT ALTITUDE $-Z_{SI}$	DESCENT ANGLE γ	INITIAL HEADING ψ_o	SINK RATE $\dot{Z}$	RADIUS OF HELIX	ROLL ANGLE ϕ	TURN RATE $\dot{\psi}$	ROLLOUT TIME t_{SI}	FINAL TIME t_f
1	700m	100m	3°	0°	3.24 m/s	1822.m	12.2°	1.95°/s	185.0s	215.5s
2	550m	100m	3°	90°	3.24 m/s	1822.m	12.2°	1.95°/s	138.5s	169.5s
3	400m	100m	3°	180°	3.24 m/s	1822.m	12.2°	1.95°/s	92.5s	123.0s
1A	700m	100m	6°	0°	6.48 m/s	909.m	23.3°	3.89°/s	93.0s	108.0s
2A	550m	100m	6°	90°	6.48 m/s	909.m	23.3°	3.89°/s	69.5s	85.0s
3A	400m	100m	6°	180°	6.48 m/s	909.m	23.3°	3.89°/s	46.5s	61.5s
3B	500m	200m	6°	180°	6.48 m/s	909.m	23.3°	3.89°/s	46.5s	77.0s

TABLE 2.- Parametric Description of Nominal Flight Paths. (Velocity at 62 meters/second).

procedure where the designer is trying to find an optimum set of weighting parameters. This task is not trivial, but by using diagonal weighting matrices, a functional relationship between their elements and the subsequent performance can be established.

The control system was required to null out initial errors in the states, and to offset the effects of steady crosswinds. It was also desired that it not be sensitive to normal changes in the atmosphere and uncertainties in the aircraft's aerodynamics. Wind gusts and sensor noise were not considered in this study. Large initial state errors tend to demand large rapid control motions. In order to avoid this, state errors are weighed less by reducing the elements of Q and control excursions are weighed more by increasing the elements of R. However, the penalty function does not include control rates and the R matrix influences the time integral rather than the magnitude of control excursion squared. Therefore, it is not unusual to get large control excursions for relatively short time with consequent high control rates. If the Q and R matrices are well chosen, the control system will null out the initial errors slowly in a manner which will cause no passenger discomfort. As the aircraft approaches the touchdown point, the influence of the M matrix tightens up the control and acceptable values of final state errors can be achieved.

This approach worked fine until the aircraft was subjected to a crosswind. It then became apparent that control in crosswinds was a much more stringent requirement and that a tighter control was necessary. In order to reconcile the two requirements: wide bandwidth control for crosswinds and narrow bandwidth control for

large initial errors, two approaches were taken. First, high gains were used, but rate and position limits were placed on the controls. This lead to undesirable oscillatory behavior, and in some cases, instability. The rate limit on angle of attack seemed to be particularly troublesome. The second approach was to make the elements of Q and R time varying. In this method, the feedback gains are low initially, while the state errors are large. While the large errors are being nulled, the feedback gains are gradually increased and the system is reasonably tight when it approaches touchdown. This second method works well except that roll rate became excessive when the aircraft rolled out of its turn. This maneuver occurs at 100 meters altitude when high feedback gains are desirable. This problem was circumvented by imposing a rate limit on roll. The values of Q, R, and M which were finally settled upon are:

$$Q = 1/2t_f \begin{bmatrix} \delta x_Q^{-2} & 0 & 0 & 0 & 0 & 0 \\ 0 & \delta y_Q^{-2} & 0 & 0 & 0 & 0 \\ 0 & 0 & \delta Z_Q^{-2} & 0 & 0 & 0 \\ 0 & 0 & 0 & \delta V_Q^{-2} & 0 & 0 \\ 0 & 0 & 0 & 0 & \delta \gamma_Q^{-2} & 0 \\ 0 & 0 & 0 & 0 & 0 & \delta \psi_Q^{-2} \end{bmatrix}$$

$$R = 1/2t_f \begin{bmatrix} \delta \alpha_R & 0 & 0 \\ 0 & \delta \phi_R & 0 \\ 0 & 0 & \delta (T/M)_R \end{bmatrix}$$

$$M = \begin{bmatrix} \delta x_M^{-2} & 0 & 0 & 0 & 0 & 0 \\ 0 & \delta y_M^{-2} & 0 & 0 & 0 & 0 \\ 0 & 0 & \delta Z_M^{-2} & 0 & 0 & 0 \\ 0 & 0 & 0 & \delta V_M^{-2} & 0 & 0 \\ 0 & 0 & 0 & 0 & \delta \gamma_M^{-2} & 0 \\ 0 & 0 & 0 & 0 & 0 & \delta \psi_M^{-2} \end{bmatrix}$$

where the value of the elements are given by

$$\delta x_Q = 140.-85.t/t_f$$

$$\delta y_Q = 140.-131.t/t_f$$

$$\delta Z_Q = 31.-26t/t_f$$

$$\delta V_Q = 70.-49.t/t_f$$

$$\delta \gamma_Q = 3.(\pi/180.)$$

$$\delta \psi_Q = (7.-6.t/t_f)(\pi/180)$$

$$\delta \alpha_R = 3+12t/t_f$$

$$\delta \phi_R = (1.7\pi/180)(1+t/t_f)$$

$$\delta (T/M)_R = .17+.17t/t_f$$

$$\delta x_M = 55.$$

$$\delta y_M = 9.$$

$$\delta Z_M = 5.$$

$$\delta V_M = 21.$$

$$\delta \gamma_M = 2.(\pi/180)$$

$$\delta \psi_M = \pi/180$$

These weights are by no means optimally chosen. They are arrived at experimentally by using the iterative process described above.

There are several constraints imposed upon the design. To avoid passenger discomfort, angular rates should not exceed ten degrees per second and by federal regulation, roll angle cannot exceed thirty degrees. Engine thrust can be throttled between 2800 and 28,000 pounds which correspond to thrust/mass ratios of .3 and 3. meters per second squared. Final errors in the states will be a function of how well the weighting matrices are chosen, the magnitude of the initial state errors, wind velocity and direction, and of the particular flight path chosen. After the wings level maneuver the aircraft is headed north at about 62 meters/second, and since the runways are normally much longer than necessary for this aircraft, an error in x of $\pm$ 62 meters is not unreasonable. However, errors in y of greater than $\pm$ 10 meters are unacceptable. The fact that the runway is normally only 50 meters wide and the wing span is approximately 30 meters make even that error uncomfortable even though some correction will be made during flare. Errors in velocity V and flight path angle γ are best viewed in terms of sink rate $\dot{Z}$ ($\dot{Z} \approx V \sin \gamma$). This error should be kept within $\pm$ .7 meters/second and again a negative error (slower descent) is preferred. Error in heading should be kept within five degrees. An error of that size can be nulled by a decrab maneuver. The most troublesome errors in this study turned out to be in y during the six degree approaches.

Representative Landing Approach

Time histories from a representative flight are shown in figure 4. The nominal curves are shown as dotted lines and the simulated flight

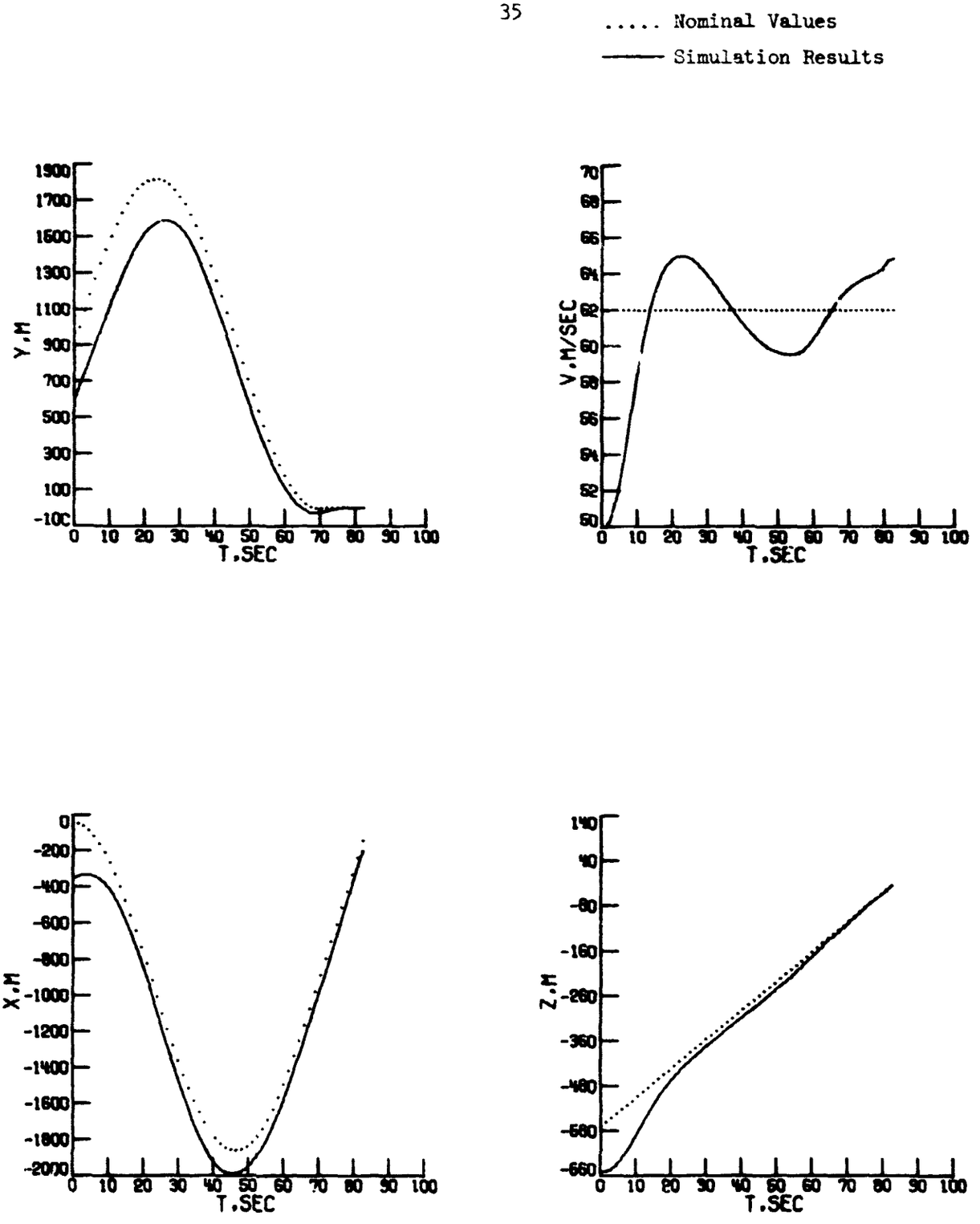

FIGURE 4.- Representative Flight, State and Control Time Histories. Flight Path 2A, Descent Angle 6°, Large Initial Errors and 15 Knot East Wind.

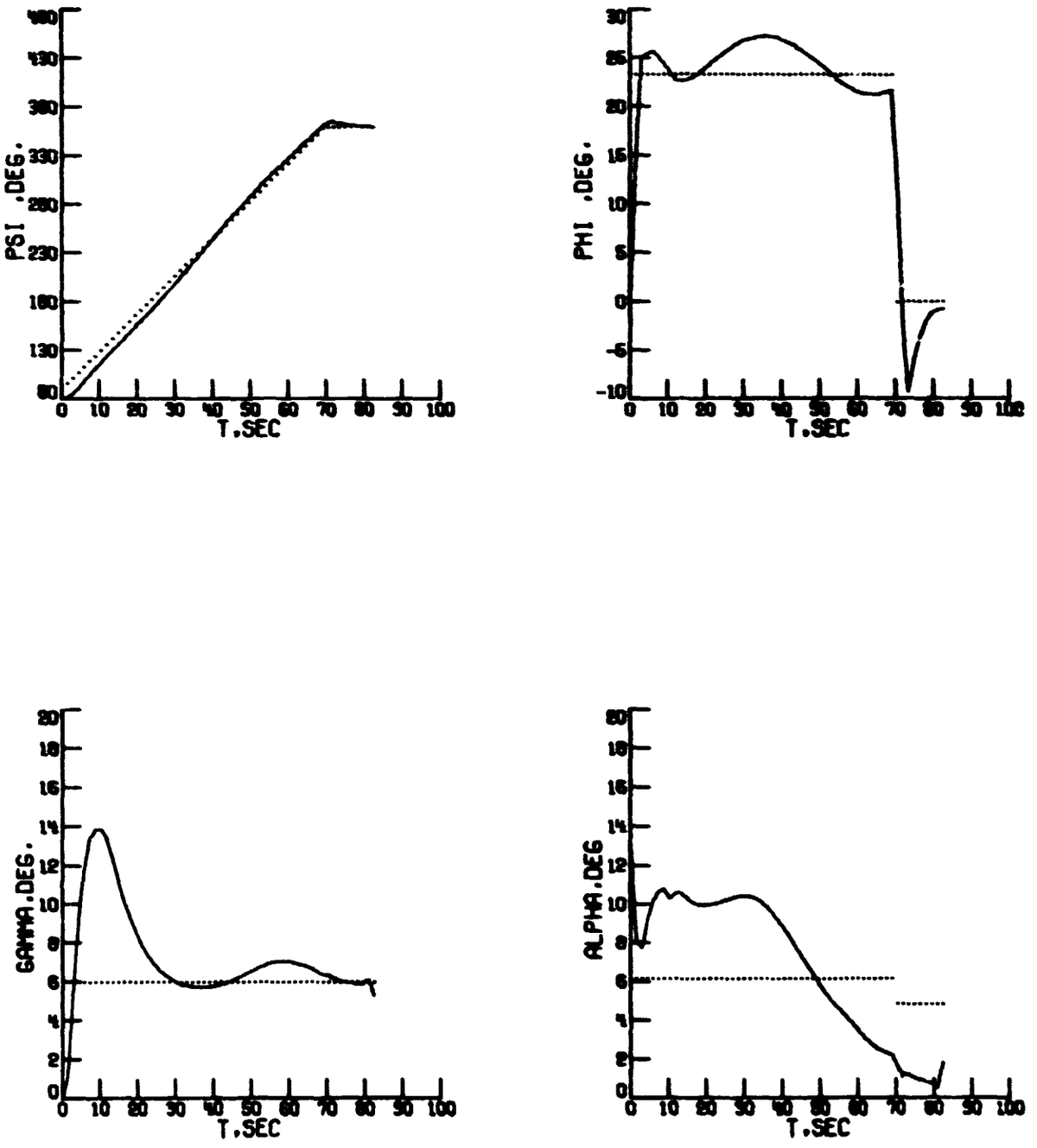

FIGURE 4.- Continued.

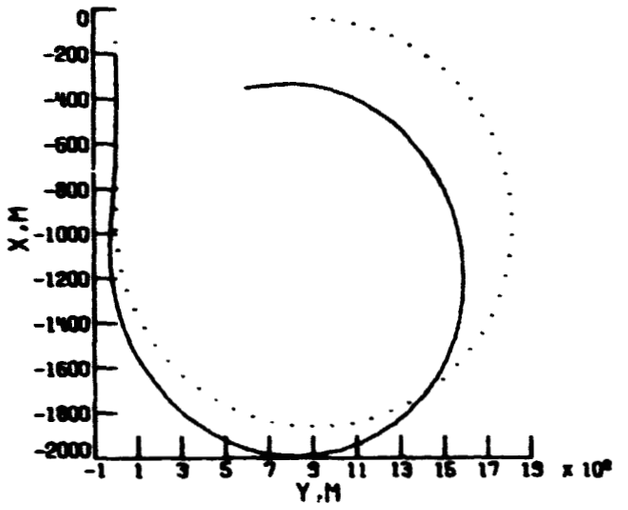

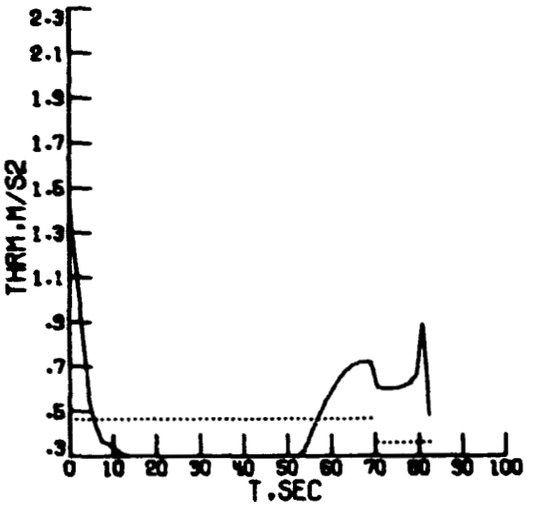

FIGURE 4.- Concluded.

as a continuous curve. This was a six degree approach with nominal initial heading due east and initial altitude of 550 meters. The six states and three controls are shown, along with an overview of the x-y plane. The aircraft started wings level with a heading of 80° (10° error). It was 100 meters higher than nominal and had over a 300 meter error in both x and y. The velocity was low by about twenty percent. The aircraft was near stall, and consequently, the angle of attack and throttle setting were set high for trim. It was subjected to a fifteen knot constant east wind. Immediately, the aircraft rolled with some overshoot to the 23° nominal. The angle of attack was decreased and the throttle was cut back. This made the aircraft simultaneously pitch over and increase speed while initiating its curved descending turn to the right. The roll-out at 100 meters altitude is apparent in the curves of y, psi, and phi. The entire approach lasted about 82 seconds and rollout occurred at around 70 seconds. The simulation was terminated when the plane reached an altitude of around 15 meters just above where the flare would be executed. Most of the motion is smooth but roll angle rate definately reaches its ten degree per second limit and the thrust to mass ratio stays on its lower limit of .3 (T = 2800 lbs.) for much of the run. The overshoot in roll angle (-10°) at rollout is undesirable, but is much less apparent in the three degree approaches. It could, most likely, be considerably reduced by making the nominal roll angle a continuous function. However, this would complicate (perhaps unjustifiably) the entire control system. At decision height, the aircraft was within one second of the nominal.

Final errors for this flight are -52m., 3m., -.6m., 3 m./s., -1°, .5°, and -.5m./s. for x, y, Z, V, γ, ψ, and $\dot{Z}$, respectively.

Representative Feedback Gains

The elements of the feedback gain matrix, K, for flight path 2A are shown in Figure 5. The magnitude of the gains, in general, increase with time due to the time variation of the weighting matrices Q and R. Some of the gains have a pronounced increase in the last several seconds of flight due to the influence of the M matrix. This can be seen in several of the elements including K(1,1), K(2,2), and K(3,3). During the straight-in portion of the approach, ten of the eighteen gains are zero or can be considered zero. Of course, the more of these elements that are zero or near zero, the easier it is to implement the control system. In order to determine the influence of a particular gain, one assumes a large reasonable error in the state and then calculates the resulting change in the control. If the change is insignificant, then the element can be considered zero. For example, an error of three meters in Z near the end of the flight would only change the thrust/mass ratio by .06. Whereas an error in x of 60 meters would cause the ratio to change by 1.2. Since these are both large reasonable errors at the termination of flight, the element K(3,3) should be considered zero. Using this approach, it can be seen that after rollout, thrust/mass ratio is a function only of x and V, roll angle is a function of only y and ψ, and angle of attack is a function of x, V, Z, and γ. This partial decoupling is useful to the designer in the iterative process of

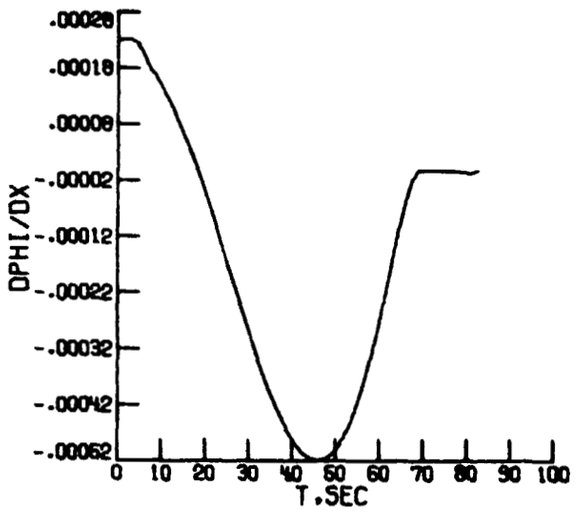

K(2,1), $\frac{\partial\phi}{\partial x}$, 1/m

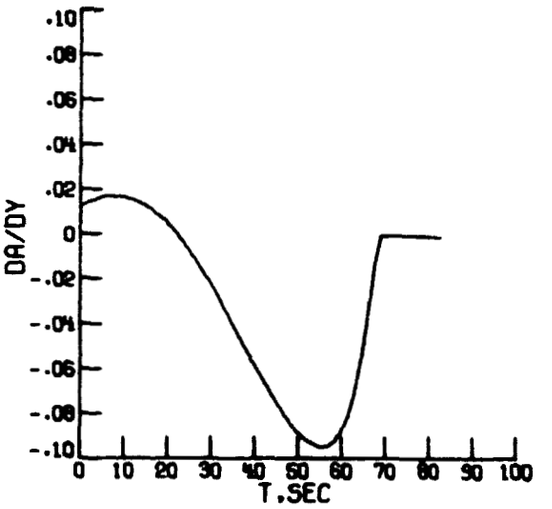

K(1,2), $\frac{\partial\alpha}{\partial y}$, Deg./m

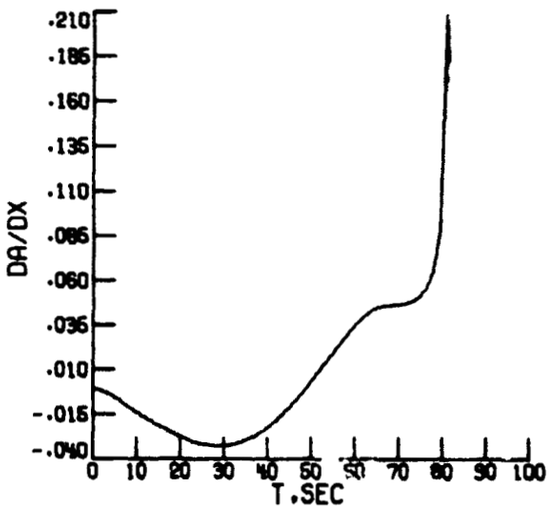

K(1,1), $\frac{\partial\alpha}{\partial x}$, Deg./m

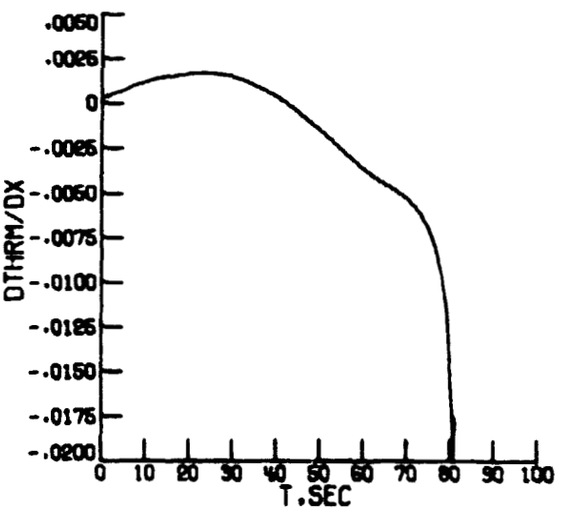

K(3,1), $\frac{\partial(T/m)}{\partial x}$, $1/s^2$

FIGURE 5.- Feedback Gains for Flight Path 2A. $\gamma = 6^\circ$, $\psi_0 = 90^\circ$, $h_0 = 550$ m.

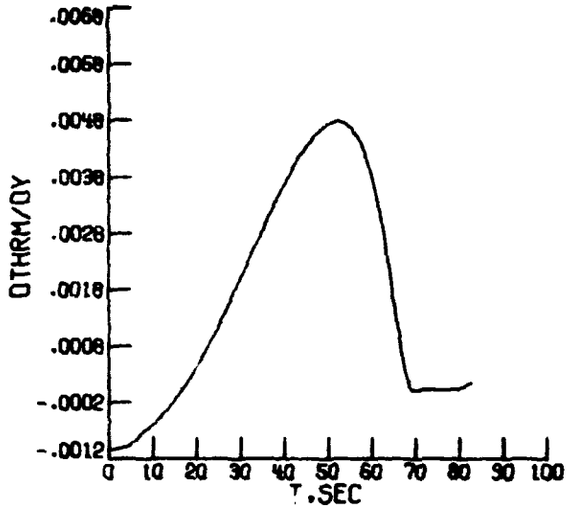

K(3,2), $\frac{\partial(T/m)}{\partial y}$, $1/s^2$

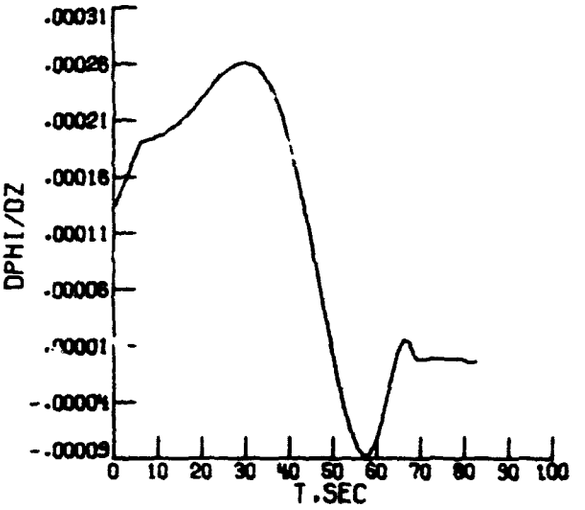

K(2,3), $\frac{\partial\phi}{\partial z}$, $1/m$

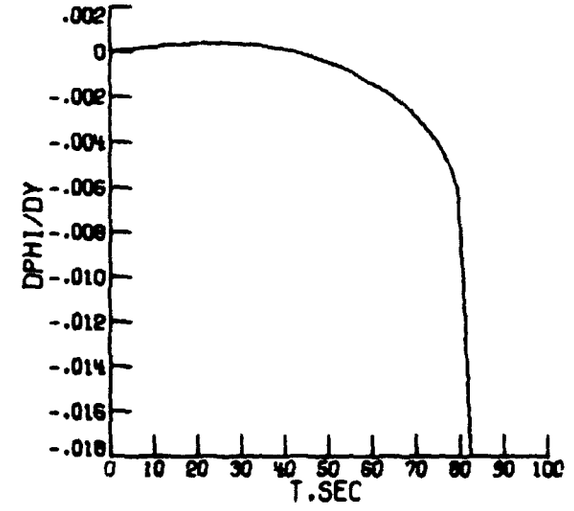

K(2,2), $\frac{\partial\phi}{\partial y}$, $1/m$

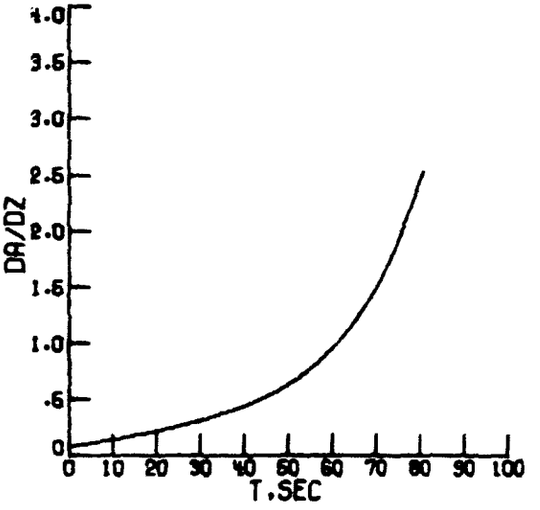

K(1,3), $\frac{\partial\alpha}{\partial z}$, Deg./m

FIGURE 5.- Continued.

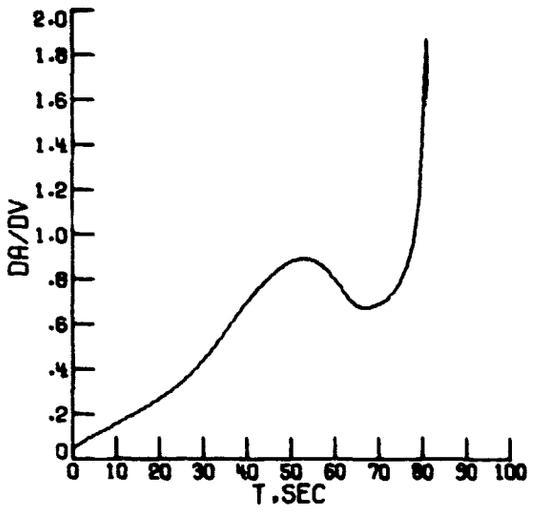

K(1,4), $\frac{\partial \alpha}{\partial V}$, Deg.-s/m

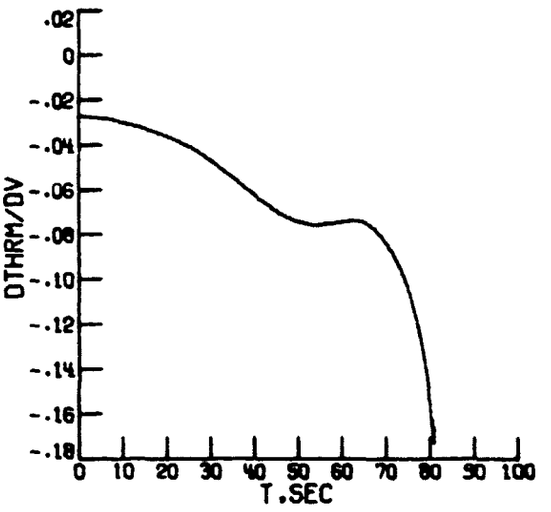

K(3,4), $\frac{\partial (T/m)}{\partial V}$, 1/s

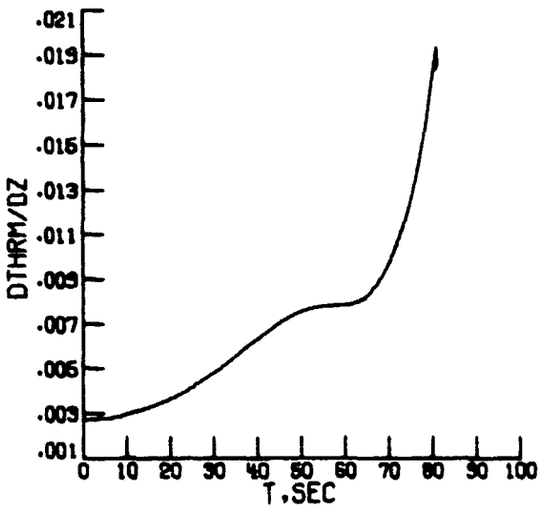

K(3,3), $\frac{\partial (T/m)}{\partial z}$, $1/s^2$

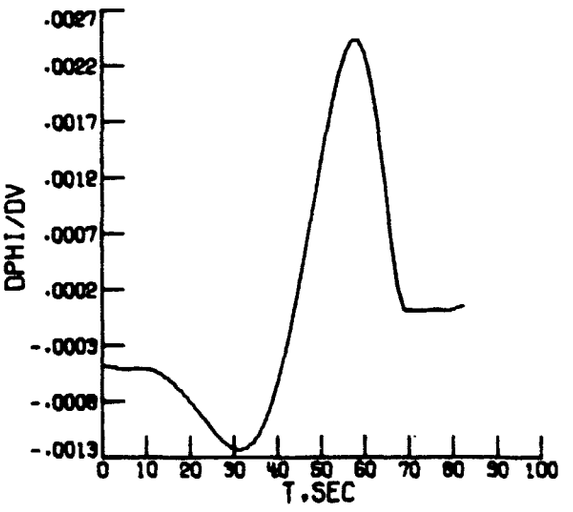

K(2,4), $\frac{\partial \phi}{\partial V}$, s/m

FIGURE 5.- Continued.

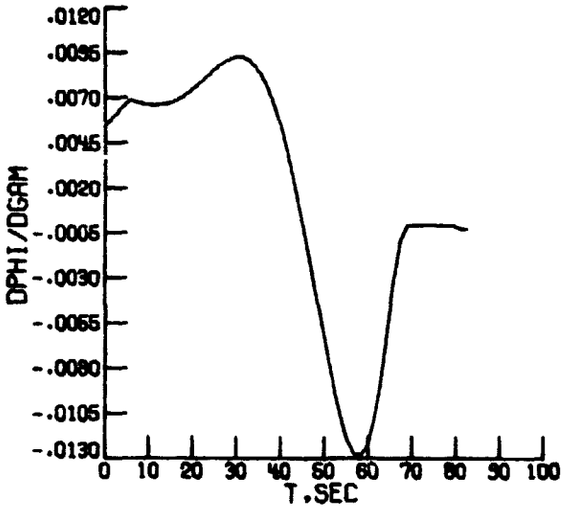

K(2,5), $\frac{\partial \phi}{\partial \gamma}$

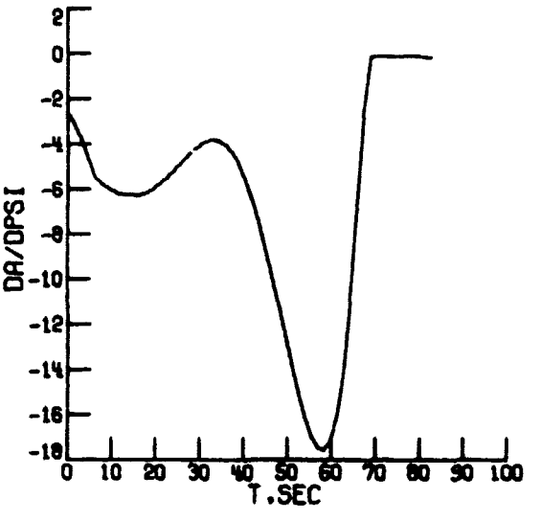

K(1,6), $\frac{\partial \alpha}{\partial \psi}$, Deg.

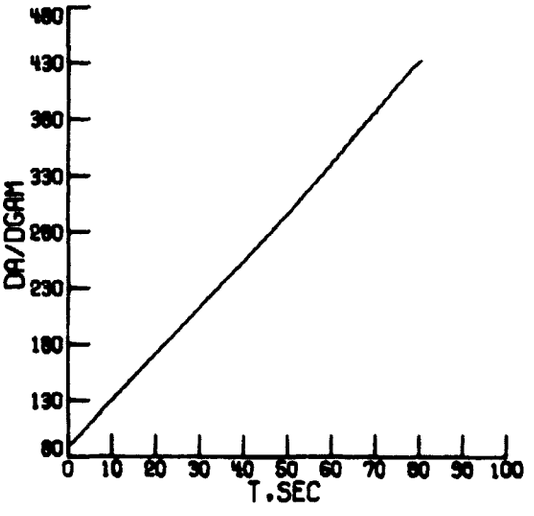

K(1,5), $\frac{\partial \alpha}{\partial \gamma}$, Deg.

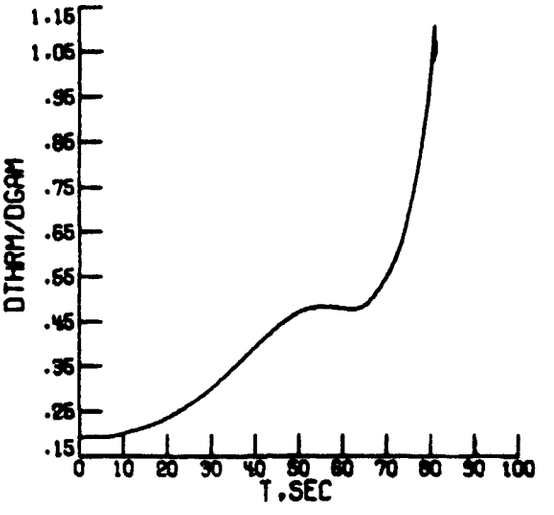

K(3,5), $\frac{\partial (T/m)}{\partial \gamma}$, m/s^2

FIGURE 5.- Continued

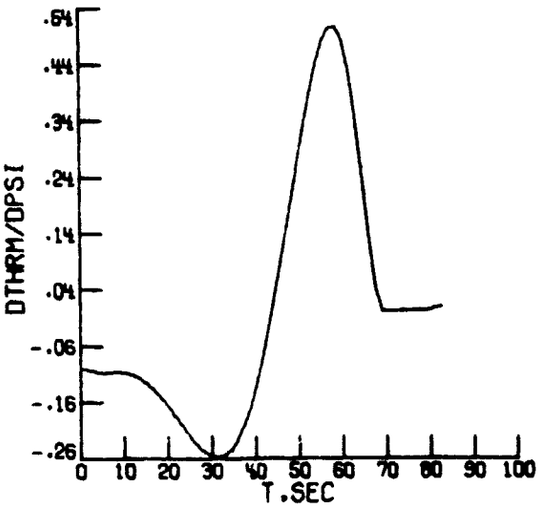

K(3,6), $\frac{\partial(T/m)}{\partial\psi}$, m/s^2

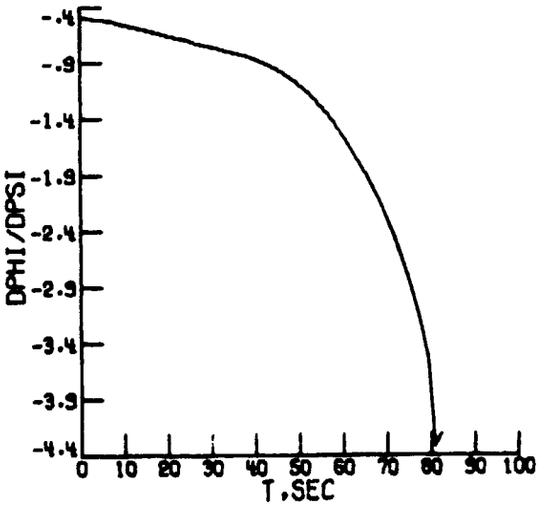

K(2,6), $\frac{\partial\phi}{\partial\psi}$

FIGURE 5.- Concluded.

choosing the weighting matrices. Applying the same reasoning, five elements of K can be considered zero throughout the entire flight. They are K(2,3), K(2,4), K(2,5), K(3,5), and K(3,6). Each of the remaining 13 gains would have to be stored in the on-board computer. Eleven points with linear interpolation could easily approximate any of these functions. Some of them could be fitted by low order polynomials in time which would require even less parameter storage. It appears that the entire gain matrix and nominal path could be stored in less than two hundred words of storage. This number could probably be reduced but it is important to realize that any parameter change in the nominal state trajectory will affect these gains. Each airport using this system would probably have several different nominal approaches and these would also probably differ among airports. To be practical then, the computer must have access to the correct set of parameters out of many possible alternative sets. Several possible ways of accomplishing this are:

1) All necessary parameter sets are stored in an on-board mass storage device.
2) The particular set of parameters needed is calculated on the airborne computer prior to landing approach.
3) The parameter set is transmitted from the airport to the on-board computer when the landing approach is assigned.
4) The feedback gains could possibly be expressed as analytic functions of time and the five primary parameters of the nominal flight path.

The feedback gains of Figure 5 were calculated using the weighting matrices M, Q, and R as given above. The gains were used in the landing approach shown in Figure 4. This choice of weighting matrices and resulting gains appears adequate for this flight path and control task.

System Performance

The control system was tested on each of the seven landing approaches described in Table 2. Results from the first six flight paths are given in Table 3 through Table 8. Flight path 3B results are given in Table 9. Each of these seven tables represent 25 simulated landing approaches. On each approach, the aircraft was subjected to a constant wind of 15 knots magnitude from a direction ψ_ω. The direction changed for each approach and it was generated as a random variable with uniform distribution between -180 degrees and +180 degrees. Each flight path had its own random sequence of wind directions with no particular direction being favored. Each approach was started with off nominal errors in all state variables. These initial errors were generated as random variables. They were normally (Gaussian) distributed with zero mean. The standard deviations selected for the six state errors in x, y, Z, V, γ, ψ, respectively, were 100m., 100m., 30m., 3m./s., [illegible], and 3°. Each flight path had a distinct random sequence of sets of initial state errors.

The reason for employing randomness in the control task was that the system showed that it could be tuned to a particular task. Originally, only 90° crosswinds were used because they were thought to be a worse case. Then it was discovered that winds from the aft

quarter occasionally gave more trouble. Because this aircraft is relatively clean; i.e., high lift to drag ratio, these winds were particularly difficult on the steep approaches. Also, certain combinations of initial errors were easier to correct than others. Therefore, a strong wind randomly directed was used and the aircraft was initialized with large random off-nominal errors. The controls were initially set such that the wings were level ($\phi = 0$) and the aircraft was trimmed.

Table 3 presents the data for the 25 landing approaches along flight path one. The first six lines give the measured statistics of the initial state errors. They are the mean, standard deviation, and range of initial errors given for each state. These statistics differ from their ideal values because they represent a subset of a very long pseudo random sequence which has the selected statistics. The next three lines of the table represent the initial off-nominal values of the controls. These are not really errors, but show a variation in initial trim values. Roll angle is a constant -12.2° since the approach always starts wings level rather than rolled over at 12.2°. The next section of the table shows how well the control system did its work. It gives the final off-nominal errors taken just above the flare altitude. Statistics are given on the six state variables and sink rate, $\dot{Z}$. As can be seen, the control system worked very well on flight path one. Poor performance usually makes itself apparent in final errors in y and Z. For these twenty-five runs, the approaching aircraft was never more than .7 meters from the center line of the runway and the final error in altitude was never greater than 1.1 meters. Since the nominal sink rate is 3.24 meters/second, the maximum error in final altitude corresponds to

Variable	Mean	Standard Deviation	Range
	INITIAL OFF-NOMINAL ERRORS		
x (m)	-6.9	64.7	(-146., 119.)
y (m)	-13.0	84.5	(-153., 193.)
Z (m)	-4.1	32.1	(-85., 76.)
V (m/s)	.6	2.8	(-4.2, 5.2)
γ (deg)	.2	.8	(-1.3, 1.9)
ψ (deg)	.5	3.1	(-6.1, 8.6)
α (deg)	.1	1.4	(-2.1, 2.7)
ϕ (deg)	-12.2	0	
T/m (m/s^2)	-.05	.14	(-.36, .20)
	FINAL OFF-NOMINAL ERRORS (AT DECISION ALTITUDE)		
x (m)	-9.3	7.8	(-21.2, -1.0)
y (m)	.4	.2	(.3, .7)
Z (m)	.0	.6	(-.6, 1.1)
V (m/s)	.2	.5	(-.3, .9)
γ (deg)	-.0	.3	(-.5, .4)
ψ (deg)	-.1	.1	(-.2, -.1)
Ż (m/s)	-.01	.34	(-.47, .44)
	EXTREME OFF-NOMINAL EXCURSIONS DURING EACH FLIGHT		
α (deg)	4.5	.5	(3.3, 5.7)
ϕ (deg)	-.4	2.3	(-2.3, 3.9)
T/m (m/s^2)	.08	.18	(-.35, .30)
	EXTREME CONTROL RATE DURING EACH FLIGHT		
$\dot{\alpha}$ (deg/s)	.4	1.5	(-2.7, 3.4)
$\dot{\phi}$ (deg/s)	7.9	3.1	(-6.7, 9.4)
$\dot{T}$/m (m/s^3)	.00	.11	(-.21, .22)

NUMBER OF UNACCEPTABLE FLIGHTS = 0

TABLE 3.- Statistical Data From Flight Path 1.
25 Landing Approaches, γ=3°, $\dot{Z}$=3.24 m/s, V_w=15 knots, ψ_w=U[-180°, 180°], t_f=211.5s, h_f=13.7m, x_f=-262m.

Variable	Mean	Standard Deviation	Range
	INITIAL OFF-NOMINAL ERRORS		
x (m)	8.4	118.1	(-292., 236.)
y (m)	10.5	93.9	(-199., 179.)
Z (m)	2.3	21.5	(-27., 48.)
V (m/s)	.2	2.7	(-4.8, 6.9)
γ (deg)	.2	.9	(-1.4, 2.9)
ψ (deg)	-.9	2.2	(-5.7, 3.0)
α (deg)	.1	1.3	(-2.9, 2.8)
ϕ (deg)	-12.2	0	
T/m (m/s^2)	-.06	.14	(-.46, .19)
	FINAL OFF-NOMINAL ERRORS (AT DECISION ALTITUDE)		
x (m)	-8.9	6.8	(-22.9, -.4)
y (m)	.5	.2	(.2, .8)
Z (m)	-.1	.6	(-.7, 1.2)
V (m/s)	.2	.3	(-.3, .9)
γ (deg)	-.0	.2	(-.5, .4)
ψ (deg)	-.1	.1	(-.2, .0)
$\dot{Z}$ (m/s)	-.02	.29	(-.48, .44)
	EXTREME OFF-NOMINAL EXCURSIONS DURING EACH FLIGHT		
α (deg)	2.9	3.2	(-3.7, 6.6)
ϕ (deg)	4.2	.1	(4.1, 4.4)
T/m (m/s^2)	.06	.17	(-.35, .29)
	EXTREME CONTROL RATE DURING EACH FLIGHT		
$\dot{\alpha}$ (deg/s)	.5	2.0	(-3.0, 4.8)
$\dot{\phi}$ (deg/s)	8.8	.7	(6.7, 9.4)
$\dot{T}$/m (m/s^3)	.01	.15	(-.29, .23)

NUMBER OF UNACCEPTABLE FLIGHTS = 0

TABLE 4.- Statistical Data From Flight Path 2.
25 Landing Approaches, γ=3°, $\dot{Z}$=3.24 m/s, V_w=15 knots,
ψ_w=U[-180°, 180°], t_f=165.s, h_f=14.6m, x_f=-279.m

Variable	Mean	Standard Deviation	Range
	INITIAL OFF-NOMINAL ERRORS		
x (m)	11.1	95.2	(-176., 174.)
y (m)	-12.8	104.1	(-209., 217.)
Z (m)	-2.5	30.8	(-48., 73.)
V (m/s)	-.0	2.1	(-3.7, 5.2)
γ (deg)	-.1	1.1	(-1.8, 1.8)
ψ (deg)	.4	2.5	(-4.1, 6.2)
α (deg)	-.1	1.0	(-2.4, 1.8)
ϕ (deg)	-12.2	0	
T/m (m/s^2)	-.02	.20	(-.35, .29)
	FINAL OFF-NOMINAL ERRORS (AT DECISION ALTITUDE)		
x (m)	-8.8	9.3	(-26.0, 2.2)
y (m)	.6	.3	(.0, 1.3)
Z (m)	.1	.5	(-.5, 1.0)
V (m/s)	.1	.6	(-.7, 1.2)
γ (deg)	.0	.2	(-.2, .4)
ψ (deg)	-.1	.1	(-.3, -.0)
$\dot{Z}$ (m/s)	.06	.26	(-.25, .53)
	EXTREME OFF-NOMINAL EXCURSIONS DURING EACH FLIGHT		
α (deg)	2.8	3.1	(-3.8, 7.2)
ϕ (deg)	7.2	.2	(6.9, 7.5)
T/m (m/s^2)	.08	.19	(-.20, .39)
	EXTREME CONTROL RATE DURING EACH FLIGHT		
$\dot{\alpha}$ (deg/s)	-.2	1.8	(-3.5, 2.6)
$\dot{\phi}$ (deg/s)	8.3	.9	(6.4, 9.4)
$\dot{T}$/m (m/s^3)	-.00	.13	(-.24, .20)

NUMBER OF UNACCEPTABLE FLIGHTS = 0

TABLE 5.- Statistical Data From Flight Path 3.
25 Landing Approaches, γ=3°, $\dot{Z}$=3.24 m/s, V_w=15 knots
ψ_w=U[-180°, 180°], t_f=118.5s, h_f=15.5m, x_f=-296m.

Variable	Mean	Standard Deviation	Range
	INITIAL OFF-NOMINAL ERRORS		
x (m)	27.4	112.7	(-219., 276.)
y (m)	13.3	106.0	(-224., 237.)
Z (m)	-7.7	26.7	(-60., 40)
V (m/s)	-.1	3.6	(-7.2, 6.4)
γ (deg)	.1	1.1	(-1.5, 2.4)
ψ (deg)	-.3	3.3	(-6.8, 6.3)
α (deg)	-.5	1.9	(-3.4, 3.7)
ϕ (deg)	-23.3	0	
T/m (m/s^2)	-.07	.11	(-.17, .17)
	FINAL OFF-NOMINAL ERRORS (AT DECISION ALTITUDE)		
x (m)	-10.0	9.4	(-23.6, 8.3)
y (m)	8.1	.7	(6.6, 9.1)
Z (m)	-.6	.6	(-1.2, .7)
V (m/s)	.0	.5	(-1.1, .8)
γ (deg)	.1	.2	(-.2, .3)
ψ (deg)	-1.8	.2	(-2.0, -1.4)
Ż (m/s)	.11	.25	(-.36, .46)
	EXTREME OFF-NOMINAL EXCURSIONS DURING EACH FLIGHT		
α (deg)	3.1	3.8	(-3.7, 8.4)
ϕ (deg)	19.3	.1	(19.0, 19.5)
T/m (m/s^2)	.17	.14	(-.17, .35)
	EXTREME CONTROL RATE DURING EACH FLIGHT		
$\dot{\alpha}$ (deg/s)	.1	2.1	(-3.4, 3.3)
$\dot{\phi}$ (deg/s)	-10.0	0	
$\dot{T}$/m (m/s^3)	.01	.10	(-.18, .21)

NUMBER OF UNACCEPTABLE FLIGHTS = 0

TABLE 6.- Statistical Data From Flight Path 1A.
25 Landing Approaches. γ=6°, $\dot{Z}$=6.28 m/s, V_w=15 knots
ψ_w=U[-180°, 180°], t_f=105.5s, h_f=19.5m, x_f=-186m.

Variable	Mean	Standard Deviation	Range
	INITIAL OFF-NOMINAL ERRORS		
x (m)	-9.7	89.2	(-235., 147.)
y (m)	20.8	75.4	(-143., 192.)
Z (m)	1.2	26.2	(-41., 56.)
V (m/s)	.3	3.4	(-6.9, 6.2)
γ (deg)	-.0	.8	(-2.1, 1.4)
ψ (deg)	-.3	2.5	(-3.5, 6.9)
α (deg)	-.9	1.7	(-3.6, 3.2)
ϕ (deg)	-23.3	0	
T/m (m/s^2)	-.07	.11	(-.17, .24)
	FINAL OFF-NOMINAL ERRORS (AT DECISION ALTITUDE)		
x (m)	-4.9	9.0	(-25.4, 7.9)
y (m)	8.4	1.3	(6.5, 10.6)
Z (m)	-.4	1.0	(-1.7, 1.3)
V (m/s)	-.3	.5	(-1.1, .9)
γ (deg)	.0	.3	(-.4, .4)
ψ (deg)	-1.7	.3	(-2.1, -1.3)
$\dot{Z}$ (m/s)	.01	.25	(-.38, .33)
	EXTREME OFF-NOMINAL EXCURSIONS DURING EACH FLIGHT		
α (deg)	3.0	3.5	(-4.3, 6.5)
ϕ (deg)	13.3	.3	(12.8, 14.1)
T/m (m/s^2)	.09	.15	(-.16, .26)
	EXTREME CONTROL RATE DURING EACH FLIGHT		
$\dot{\alpha}$ (deg/s)	-.1	2.0	(-3.3, 3.9)
$\dot{\phi}$ (deg/s)	-10.0	0.	
$\dot{T}$/m (m/s^3)	-.01	.11	(-.17, .21)

NUMBER OF UNACCEPTABLE FLIGHTS = 5

TABLE 7.- Statistical Data From Flight Path 2A.
25 Landing Approaches. γ=6°, $\dot{Z}$=6.28 m/s, V_w=15 knots
ψ_w=U[-180°, 180°], t_f=82.5s, h_f=15.3m, x_f=-146.m.

Variable	Mean	Standard Deviation	Range
	INITIAL OFF-NOMINAL ERRORS		
x (m)	-35.6	88.4	(-225., 129.)
y (m)	-22.2	89.5	(-266., 81.)
Z (m)	-5.2	36.3	(-61., 54.)
V (m/s)	.1	2.5	(-6.0, 4.2)
γ (deg)	.1	.9	(-1.3, 2.3)
ψ (deg)	-.3	2.8	(-5.4, 4.7)
α (deg)	-1.1	1.3	(-3.0, 2.4)
ϕ (deg)	-23.3	0.	
T/m (m/s^2)	-.07	.09	(-.17, .09)
	FINAL OFF-NOMINAL ERRORS (AT DECISION ALTITUDE)		
x (m)	-21.5	14.7	(-51.7, 2.4)
y (m)	11.2	5.5	(-6.1, 20.3)
Z (m)	-.5	.7	(-1.8, 1.2)
V (m/s)	1.1	1.0	(-.8, 2.8)
γ (deg)	.1	.2	(-.4, .3)
ψ (deg)	-2.1	1.1	(-4.0, 1.4)
$\dot{Z}$ (m/s)	.17	.25	(-.22, .57)
	EXTREME OFF-NOMINAL EXCURSIONS DURING EACH FLIGHT		
α (deg)	.5	4.2	(-4.2, 7.4)
ϕ (deg)	21.7	1.0	(19.7, 23.4)
T/m (m/s^2)	.19	.21	(-.17, .55)
	EXTREME CONTROL RATE DURING EACH FLIGHT		
$\dot{\alpha}$ (deg/s)	1.1	1.8	(-2.0, 5.1)
$\dot{\phi}$ (deg/s)	-10.0	0.	
$\dot{T}$/m (m/s^3)	.02	.09	(-.15, .15)

NUMBER OF UNACCEPTABLE FLIGHTS = 14

TABLE 8.- Statistical Data From Flight Path 3A.
25 Landing Approaches. γ=6°, $\dot{Z}$=6.28 m/s, V_w=15 knots
ψ_w=U[-180°, 180], t_f=59.0s, h_f=15.m, x_f=-140m.

about one third of a second in time. This same observation can be made with regard to x since nominal $\dot{x}$ is approximately 62 meters/second and the maximum final error in x for the twenty-five runs was 21.2 meters. The third section of the table indicates how much control was needed to fly the aircraft. For each of the twenty-five approaches, the largest off-nominal control excursion is identified whether it be positive or negative. The initial transient of each run was not included since the initial off-nominal values of at least roll angle would always be extreme for the flight and it would mask the desired information. So, for example, the average extreme for angle of attack was 4.5 degrees greater than the nominal and the extreme varied over the twenty-five flights from 3.3 degrees to 5.7 degrees above nominal. The next section of the table gives information on extreme control rates for each run. These are important mainly in how they affect passenger comfort. The statistics given are on the extremes of each flight including the initial transient. Finally, the table gives the number of flights which were unacceptable because one or more of the constraints, discussed in the section on design consideration, was violated.

As can be seen from examining the tables, the control system was quite effective on flight paths 1, 2, and 3. The largest final errors for these 75 approaches was 1.3 meters in y and 1.2 meters in Z. There were no unacceptable flights and both control excursion and control rates were moderate.

The next three tables, 6 through 8, show the results for the six degree approaches. As can be seen, the control system did not

do as well on these approaches. Final errors in y and ψ were larger, and roll angle tended to have larger off-nominal excursions. Although there were no unacceptable flights on path 1A, the mean final error in y was a disturbing 8.1 meters. Because the aircraft did not execute the wings level maneuver fast enough, it tended to go off to the right (east), and then it would roll to the left in order to get back on the centerline. On these six degree approaches, there was only about 13 seconds from initiation of rollout to the conclusion of the simulation. Since the variation of the error is small (.7), performance on this flight path could probably be improved by starting the rollout a few seconds early. This is, in fact, what pilots have been observed to do when flying this approach. On flight path 2A, performance is slightly worse and five of these had final errors in y which were greater than ten meters and consequently were unacceptable. The variation in final y error was again small, indicating that a slight adjustment in the flight path could possibly bring the errors within plus or minus 2.5 meters. Finally, on flight path 3A, the control system proved to be completely inadequate with 14 of the 25 flights having final errors in y which were greater than ten meters. It is possible that another choice of weights, specifically δy_Q and δy_M, might improve performance on the six degree flight paths. However, the principle problem seems to be one of time. Flight time decreases monotonically from 212 seconds on flight path 1 to around 60 seconds on flight path 3A. It appears that the six degree approaches do not have enough time to null out initial errors and the adverse effect of crosswinds. In

order to support this premise, flight path 3A was modified such that initial altitude was 500 meters instead of 400, and rollout was accomplished at 200 meters instead of 100. This new flight path is labeled 3B. Its parameters are given in Table 2 and its performance is reported in Table 9. In order to facilitate comparison of Table 9 and Table 8, the exact same sequences of initial errors and wind directions were used. The flight time for 3B was about 15 seconds longer than 3A, and all of this was added to the straight-in portion of the flight. The marked improvement in performance of 3B over 3A is apparent when Table 9 is compared with Table 8. On 3B, no approach exceeded the allowable limit of ten meters final error in y; whereas on 3A, 14 approaches exceeded it. Since this improvement seems to be caused by the increased flying time, it may follow that doubling the initial nominal altitude and rollout altitude on the six degree approaches would lead to performance comparable to that experienced on the three degree approaches.

Finally, the control system was tested for sensitivity to uncertainties in the aerodynamics of the aircraft and for normal variation in the atmosphere. A particular landing approach was used. Initial errors and wind direction were not varied. Twenty-five simulation runs were made, each with a different atmospheric density function and each with a different set of aerodynamic parameters. The results of these flights are given in Table 10. All six aircraft parameters were allowed to vary randomly. The values given in Table 1 were used as the mean and four percent of those values were used as the standard deviation. The distribution was normal. This resulted

Variable	Mean	Standard Deviation	Range
	INITIAL OFF-NOMINAL ERRORS		
x (m)	-35.6	88.4	(-225., 129.)
y (m)	-22.2	89.5	(-266., 81.)
Z (m)	-5.2	36.3	(-61., 54.)
V (m/s)	.1	2.5	(-6.0, 4.2)
γ (deg)	.1	.9	(-1.3, 2.3)
ψ (deg)	-.3	2.8	(-5.4, 4.7)
α (deg)	-.9	1.3	(-2.9, 2.6)
ϕ (deg)	-23.3	0.	
T/m (m/s^2)	- .7	.09	(-.17, .09)
	FINAL OFF-N ' L ERRORS (AT DECISION ALTITUDE)		
x (m)	-16.2	14.2	(-42.4, 13.2)
y (m)	4.8	2.1	(-.6, 8.5)
Z (m)	-.7	.5	(-1.4, .6)
V (m/s)	.8	.6	(-.4, 2.1)
γ (deg)	.0	.2	(-.6, .3)
ψ (deg)	-.8	.3	(-1.4, .1)
$\dot{Z}$ (m/s)	.12	.3	(-.54, .50)
	EXTREME OFF-NOMINAL EXCURSIONS DURING EACH FLIGHT		
α (deg)	.9	4.1	(-4.1, 7.2)
ϕ (deg)	21.6	.8	(19.6, 23.1)
T/m (m/s^2)	.18	.19	(-.17, .46)
	EXTREME CONTROL RATE DURING EACH FLIGHT		
$\dot{\alpha}$ (deg/s)	1.1	1.8	(-2.0, 5.0)
$\dot{\phi}$ (deg/s)	-10.0	0.	
$\dot{T}$/m (m/s^3)	.0	.1	(-.15, .15)

NUMBER OF UNACCEPTABLE FLIGHTS = 0

TABLE 9.- Statistical Data From Flight Path 3B.
25 Landing Approaches. γ=6°, $\dot{Z}$=6.28 m/s, V_w=15 knots
ψ_w=U[-180°, 180°], t_f=75.0s, h_f=14.7m, x_f=-135m.

Variable	Mean	Standard Deviation	Range
	INITIAL OFF-NOMINAL ERRORS		
x (m)	186.0		
y (m)	157.9		
Z (m)	-24.0		
V (m/s)	1.4		
γ (deg)	-.2		
ψ (deg)	2.1		
α (deg)	-.6		
ϕ (deg)	-12.2		
T/m (m/s^2)	.01		
	FINAL OFF-NOMINAL ERRORS (AT DECISION ALTITUDE)		
x (m)	-2.0	8.4	(-23.7, 12.4)
y (m)	.3	.1	(.2, .5)
Z (m)	1.3	.8	(-.2, 3.0)
V (m/s)	-.2	.5	(-1.1, 1.0)
γ (deg)	.4	.1	(-.0, .5)
ψ (deg)	-.1	.0	(-.1, -.1)
Ż (m/s)	.43	.1	(.05, .51)
	EXTREME OFF-NOMINAL EXCURSIONS DURING EACH FLIGHT		
·)	4.7	.8	(3.7, 7.1)
)	4.3	.0	(4.2, 4.3)
ı/s^2)	-.14	.15	(-.32, .34)
	EXTREME CONTROL RATE DURING EACH FLIGHT		
$\dot{\alpha}$ (deg/s)	-1.0	.3	(-1.3, .5)
$\dot{\phi}$ (deg/s)	8.9	.0	(8.9, 8.9)
$\dot{T}$/m (m/s^3)	-.16	.01	(-.17, 0.15)

NUMBER OF UNACCEPTABLE FLIGHTS = 0

TABLE 10.- Statistical Data From Flight Path 2 With Variations in the Aerodynamic Parameters.
25 Landing Approaches. γ=3°, $\dot{Z}$=3.24 m/s, V_w=15 knots, ψ_w=170°, t_f=165., h_f=14.6m, x_f=-279.m. Random variation of Approximately ± 10% in Aircraft Parameters and ± 5% in Air Density.

in a random variation in these parameters of about ±10%. Air density, as described in equation 7, was also given random variation. The multiplying coefficient, 1.22, of that equation was allowed to vary normally with mean 1.22 and standard deviation of .0244. This resulted in a random variation of air density of about ±5% for any particular altitude. These variations seemed only to propagate into the final errors in x, Z, and V and into the extreme control excursions in angle of attack. Of these, only the variation in the final altitude causes concern. It varies between .4 and 2.4 meters. Since the sink rate is about 3.24 meters/second, it follows that this corresponds to an error of about .6 seconds in time. The control system appears to handle these normal variations and uncertainties quite well.

CONCLUSIONS

This paper describes an application of linear optimal regulator theory to a nonlinear simulation of an aircraft performing a helical landing approach. The nonlinear equations of motion are developed and are linearized (time varying coefficients) about a quasi-steady helical flight path. The nominal state time histories are given as explicit functions of time and a numerical method for determining the constant control inputs is presented. Control of the system to the nominal state trajectories is posed as a regulator problem with time varying weighting matrices in the cost functional. A method of solving for the feedback gain matrix is reviewed. This theory is then implemented in a simulation of Boeing 737-100, and system performance was measured for seven distinct approaches including flight path angles (descent angles) of three and six degrees. On each approach, the aircraft was subject to large errors in initial values of state variables and to strong steady crosswinds. The system was also tested for sensitivity to normal variations in atmosphere and to reasonable uncertainties in the parametric description of the aircraft. Statistical data on 200 simulated landings is presented.

The control system performed very well on all the three degree approaches and was reasonably insensitive to changes in the atmosphere and to parametric changes in the aircraft model. Performance, which was measured in terms of terminal errors, violation of design constraints, and passenger comfort, was not

nearly as good on the six degree approaches. These approaches are more difficult to execute since descent rate and roll angle are doubled and the radius of the helix is halved. On the most difficult of these six degree approaches, the total flight time was about sixty seconds, and performance was definitely unacceptable. Evidence is presented to support the contention that total flight time is the critical factor and that performance on the six degree paths could be greatly improved by starting the approach from a higher altitude. This hypothesis needs to be further tested if six degree approaches are a requirement.

The control system design method used in this study is relatively straight forward and is easy to implement with the aid of a modern computer. The only difficulty is in choosing the weighting matrices for the cost functional. It was concluded in this paper that the weights should be time varying for the particular control task studied. This method should be extended to the more complex simulation which includes both actuators and sensors and has six degree of freedom dynamics before being implemented on the aircraft.

REFERENCES

1. Athans, M., and Falb, P. L. "Optimal Control, An Introduction to the Theory and Its Applications" New York: McGraw-Hill, Inc., 1966.

2. Bryson, Arthur E., and Ho, Yu-Chi. "Applied Optimal Control". Waltham: Ginn and Company, 1969.

3. Kwakernaak, Huibert, and Sivan, Raphael. "Linear Optimal Control Systems". New York: John Wiley and Sons, Inc., 1972.

4. Hsu, Jay C., and Meyer, Andrew U. "Modern Control Principles and Applications". New York: McGraw-Hill, Inc., 1968.

5. Meditch, J. S. "Stochastic Optimal Linear Estimation and Control". New York: McGraw-Hill, Inc., 1969.

6. Hoffman, William C., Zvara, John and Bryson, Arthur E. "A Landing Approach Guidance Scheme for Unpowered Lifting Vehicles". Journal of Spacecraft, Vol. 7, No. 2 (February 1970), 196-202.

7. U. S. Standard Atmosphere Supplements, 1966, U. S. Government Printing Office, Washington, D.C., 1966.

8. Burrows, James W., and Tobie, H. N. "Linear Energy Management During Unpowered Landing Approach". Report of the Boeing Company, Commercial Airplane Division, Renton, Washington, Document No. D6-24909TN, 1971.

9. Olason, M. L., and Norton, D. A. "Aerodynamic Design Philosophy of the Boeing 737". Journal of Aircraft, Vol. 3, No. 6 (November 1966), 524-528.

10. Harrison, Neil. "Boeing 737, A Short Hauler Engineered for Efficiency". Flight International (3 February 1966), 181-188.

11. Scarborough, J. B. "Numerical Mathematical Analysis". Fourth Edition. Baltimore: The Johns Hopkins Press, 1958.

12. Reeder, John P., Taylor, Robert T., and Walsh, Thomas M. "Operating Techniques for Improved Terminal Area Compatability". No. 740454, Society of Automotive Engineers, Apr. - May 1974.

APPENDIX A

JACOBIAN MATRICES USED IN THE LINEARIZATION OF THE AIRCRAFT DYNAMICS

The aircraft dynamics were linearized about a nominal state trajectory and nominal control time history. This was done in order to apply linear optimal regulator theory to the computation of the feedback gains. As is evident in equation (3) of the text, the Jacobian matrices

$$A(t) = \frac{\partial \bar{f}}{\partial \bar{x}} \quad \text{and} \quad B(t) = \frac{\partial \bar{f}}{\partial \bar{u}}$$

are needed. They are

$$\frac{\partial \bar{f}}{\partial \bar{u}} = \begin{bmatrix} 0 & 0 & 0 \\ 0 & 0 & 0 \\ 0 & 0 & 0 \\ -\left[\frac{\partial D}{\partial \alpha}/m + (t/m)\sin\alpha\right] & 0 & \alpha \\ -\left[T\cos\alpha + \frac{\partial L}{\partial \alpha}\cos\phi\right]/mV & (L/mV)\sin\phi & -\sin\alpha/V \\ \frac{\partial L}{\partial \alpha}\sin\phi/(mV\cos\gamma) & (L/mV)\cos\phi/\cos\gamma & 0 \end{bmatrix} \tag{A1}$$

where $\frac{\partial L}{\partial \alpha} = g\,S\,C_{L_\alpha}\,\frac{\pi}{180}$, $\frac{\partial D}{\partial \alpha} = 2q\,S\,C_{L_\alpha}^2\,\eta\left(\frac{\pi}{180}\right)^2(\alpha - \alpha_0)$

and

$$\frac{\partial \bar{f}}{\partial \bar{x}} = \begin{bmatrix} 0 & 0 & 0 & \cos\gamma\cos\psi & -V\sin\gamma\cos\psi & -V\cos\gamma\sin\psi \\ 0 & 0 & 0 & \cos\gamma\sin\psi & -V\sin\gamma\sin\psi & V\cos\gamma\cos\psi \\ 0 & 0 & 0 & \sin\gamma & V\cos\gamma & 0 \\ 0 & 0 & 0 & 2D/(mV) & g\cos\gamma & 0 \\ 0 & 0 & 0 & \left[(T/m)\sin\alpha - g\cos\gamma - (L/m)\cos\phi\right]V^{-2} & (g/V)\sin\gamma & 0 \\ 0 & 0 & 0 & (L/m)\sin\phi / (V^2\cos\gamma) & (L/m)\sin\phi\sin\gamma / (V\cos^2\gamma) & 0 \end{bmatrix} \quad \text{(A2)}$$

An assumption that atmospheric density is constant over the range of altitude considered is incorporated into these equations. This assumption is discussed in the text. It is not made in the non-linear simulation which uses the feedback gains.